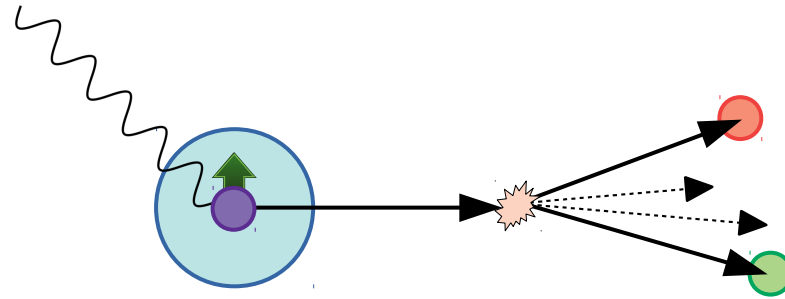


Dihadrons at the EIC



Christopher Dilks

4 May 2020

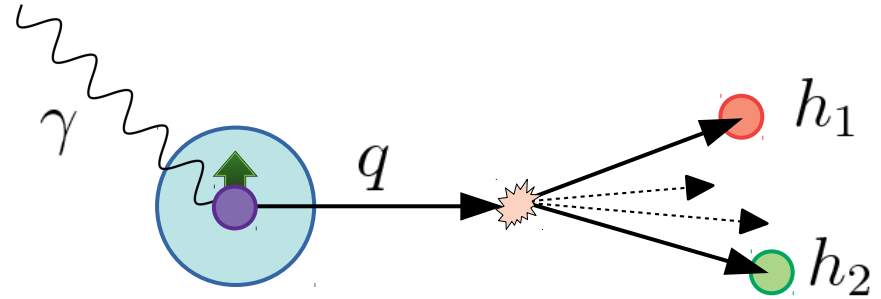
YR-SIDIS Meeting



Dihadrons: Probing Spin-Orbit Correlations in Hadronization

Unpolarized SIDIS:

- ◆ **Cahn Effect:** quark transverse momentum leads to azimuthal modulations of SIDIS cross section
- ◆ **Boer-Mulders Effect:** Non-collinear quarks in an unpolarized proton can have transverse polarization, also contributing azimuthal modulations



Boer-Mulders and Cahn effects are comparable in single hadron production

- HERMES and COMPASS data, e.g. Phys.Rev.D 81 (2010) 114026

Dihadrons can help decouple BM from Cahn

- Extra degree of freedom in dihadrons
 - Cahn effect impacts dihadron total momentum direction P_h
 - Utilize azimuthal angle about P_h , in addition to the azimuth about the virtual photon

Advantages from a broader and higher Q^2 range at an EIC

- Broader Q^2 range probes evolution effects
- Higher Q^2 suppresses Cahn effect in single-hadron asymmetries (Cahn is twist-4)
- Lower Q^2 for overlap with other SIDIS experiments

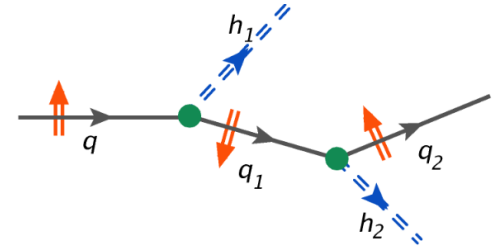
Dihadrons: Probing Spin-Orbit Correlations in Hadronization

Longitudinally polarized SIDIS:

■ Helicity DiFF G_1^\perp :

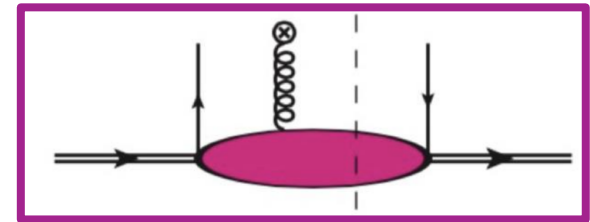
- **Not yet constrained by data!**
- **Spin-orbit correlations** in hadronization
- Fragmenting quark acquires transverse polarization via 'wormgear' splitting in the quark-jet hadronization model
- Preliminary CLAS12 data indicate **significant effect**, dependent on invariant mass

$$G_1^\perp = \text{Diagram 1} - \text{Diagram 2}$$



■ Collinear Twist-3 PDFs $e(x)$ and $h_L(x)$:

- **CLAS6 data provided the first $e(x)$ extraction, consistent with models; CLAS12 data are in agreement**
- Physical Interpretation via moments of $e(x)$:
 - **Transverse color-force** on a transversely polarized struck-quark, in an unpolarized proton
 - **πN sigma terms**:
 - Quark mass contribution to proton mass
 - Quark chromomagnetic dipole moment \rightarrow CP-odd π -N coupling
- **No experimental constraints yet for $h_L(x)$**



Transversely polarized SIDIS: Access several additional TMDs

Transverse Momentum Dependent Distributions and Fragmentation Functions

Twist-2 TMDs

QUARKS	unpolarized	chiral	transverse
U	f_1		h_1^\perp
L		g_{1L}	h_{1L}^\perp
T	f_{1T}^\perp	g_{1T}	$h_{1T}^\perp, h_{1T}^\perp$

Twist-3 TMDs

N/q	U	L	T
U	f^\perp	g^\perp	h, e
L	f_L^\perp	g_L^\perp	h_L, e_L
T	f_T, f_T^\perp	g_T, g_T^\perp	$h_T, e_T, h_T^\perp, e_T^\perp$

$e, h_L,$ and g_T are collinear

Dihadron Fragmentation Functions (DiFFs)

$h_1 h_2 / q$	U	L	T
UU	$D_{1,OO}$		$H_{1,OO}^\perp$
LU	$D_{1,OL}$		$H_{1,OL}^\perp$
LL	$D_{1,LL}$		$H_{1,LL}^\perp$
TU	$D_{1,OT}$	$G_{1,OT}^\perp$	$\begin{cases} H_{1,OT}^\perp & \text{if } m < 0 \\ H_{1,OT}^\triangleleft & \text{if } m > 0 \end{cases}$
TL	$D_{1,LT}$	$G_{1,LT}^\perp$	$\begin{cases} H_{1,LT}^\perp & \text{if } m < 0 \\ H_{1,LT}^\triangleleft & \text{if } m > 0 \end{cases}$
TT	$D_{1,TT}$	$G_{1,TT}^\perp$	$\begin{cases} H_{1,TT}^\perp & \text{if } m < 0 \\ H_{1,TT}^\triangleleft & \text{if } m > 0 \end{cases}$

Dihadron Structure Functions → PDF convolved with DiFF

$$F_{UU} \quad f_1 \otimes D_1 \quad h \otimes H_1$$

$$h_1^\perp \otimes H_1$$

$$F_{LU} \quad f_1 \otimes G_1 \quad e \otimes H_1$$

$$F_{UL} \quad g_{1L} \otimes G_1 \quad h_L \otimes H_1$$

$$h_{1L}^\perp \otimes H_1$$

$$F_{LL} \quad g_{1L} \otimes D_1 \quad e_L \otimes H_1$$

$$F_{UT} \quad f_{1T}^\perp \otimes D_1 + g_{1T} \otimes G_1 \quad f_T \otimes D_1 \quad h_T \otimes H_1$$

$$h_1 \otimes H_1 \quad f_T^\perp \otimes D_1 \quad h_T^\perp \otimes H_1$$

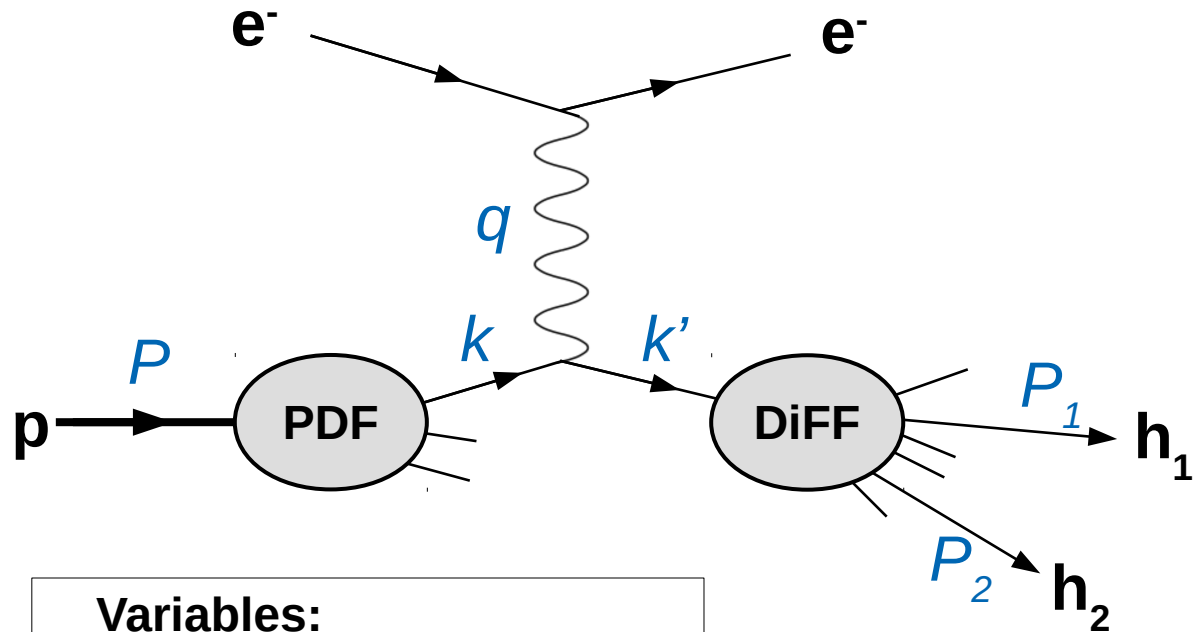
$$h_{1T}^\perp \otimes H_1$$

$$F_{LT} \quad g_{1T} \otimes D_1 + f_{1T}^\perp \otimes G_1 \quad g_T \otimes D_1 \quad e_T \otimes H_1$$

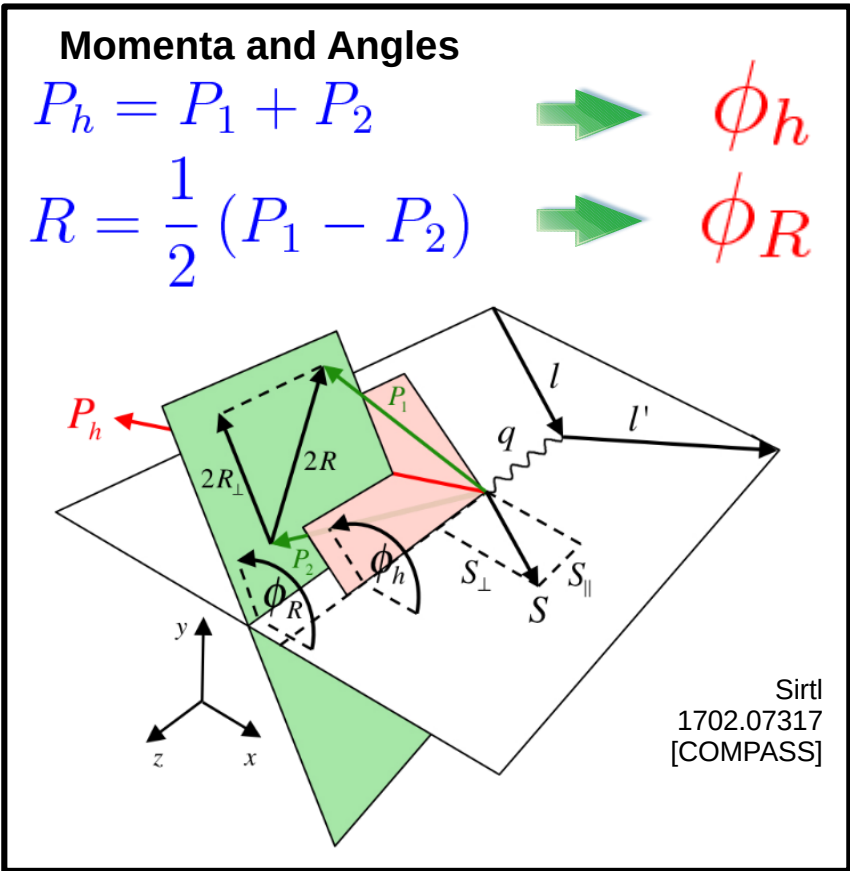
$$g_T^\perp \otimes D_1 \quad e_T^\perp \otimes H_1$$

- Dihadrons are sensitive to a zoo of PDFs and DiFFs
- Cross section modulations
 - Boer-Mulders Function
- Longitudinal spin asymmetries
 - Helicity DiFF G_1^\perp
 - Collinear Twist-3 PDFs
- Transverse Spin Asymmetries
 - Sivers, Wormgear, Transversity, Pretzelosity
 - Twist-3 TMDs
- θ -dependence → DiFF partial waves

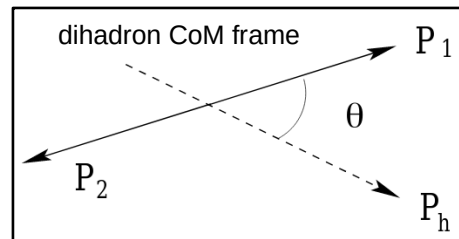
Dihadron Kinematics



- Variables:**
- Scale: Q^2
 - Bjorken-x: x
 - Feynman-x: x_F
 - Invariant Mass: M_h
 - Fragmentation fraction: z
 - Missing Mass: M_x



Dihadron CoM
production angle:



Event Selection

$Q^2 > 1 \text{ GeV}^2$ cut for event generator

$E'_e < E_e$ scattered electron has less energy than incident electron

$W > 3 \text{ GeV}$ exclude elastic / resonance region

$0.01 < y < 0.95$ lower bound is to avoid region in which calculating x , Q^2 , etc. via the e' momentum may differ from that from JB method

$x_{F_h} > 0$ ensures hadrons are produced in the current fragmentation region

$z_h > 0.01$ cuts out long M_h tail at $z \sim 0$ peak (need to think about...)

$z_{h_1 h_2} < 0.95$ helps avoid exclusive region

For Kinematic Maps, focus on $\pi^+\pi^-$

Dataset

Energies:

- 5x41 $\sqrt{s} = 28.7$ GeV
- 5x100 $\sqrt{s} = 44.7$ GeV
- 10x100 $\sqrt{s} = 63.3$ GeV
- 18x275 $\sqrt{s} = 140.7$ GeV

▣ Event Generation

- Pythia8 + DiRE (plan to switch to Pythia6+RADGEN soon)
 - 1M events
 - Radiative corrections (including QED) enabled via ``PDF:lepton=on``
 - All other parameters follow ``dis_example.cmd`` in the escalate tutorial notebook
- Kinematic maps below focus on 10x100 and 18x275

▣ Fast Simulation

- ``eic_smear`` with the ``handbook`` detector setting
- uses custom standalone eJANA plugin for production of dihadron trees

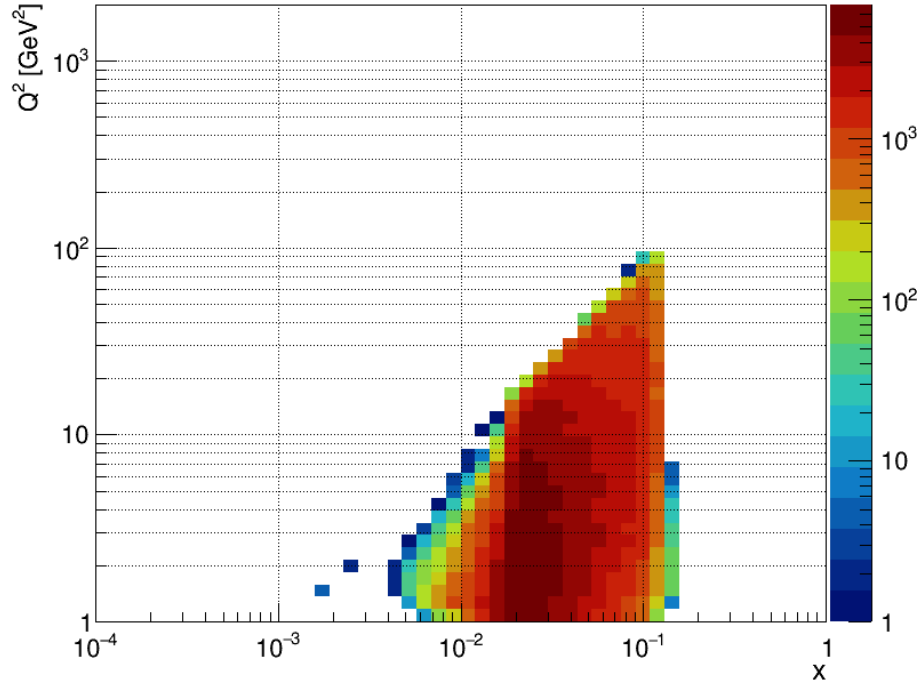
▣ Analysis

- Dihadron trees compatible with CLAS analysis code, generalized for EIC
 - Architecture for asymmetry fits / projections is ready
 - Projections for partial wave amplitudes is also possible
- Kinematic Studies
- PID studies

(x, Q^2) Plane for 5x41 and 5x100

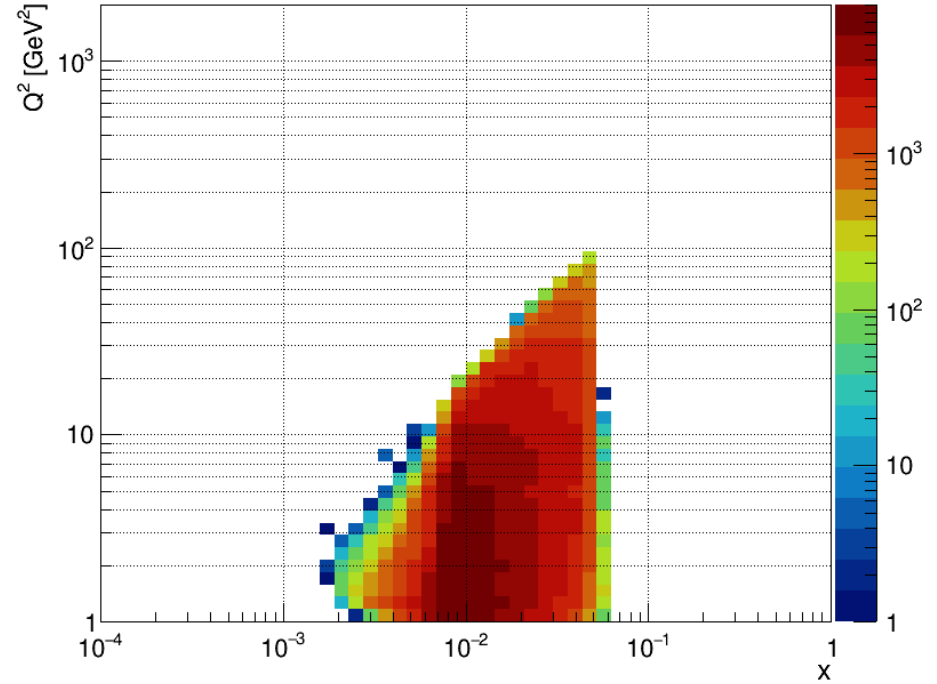
5x41 GeV

Q^2 vs. x for selected dihadrons



5x100 GeV

Q^2 vs. x for selected dihadrons

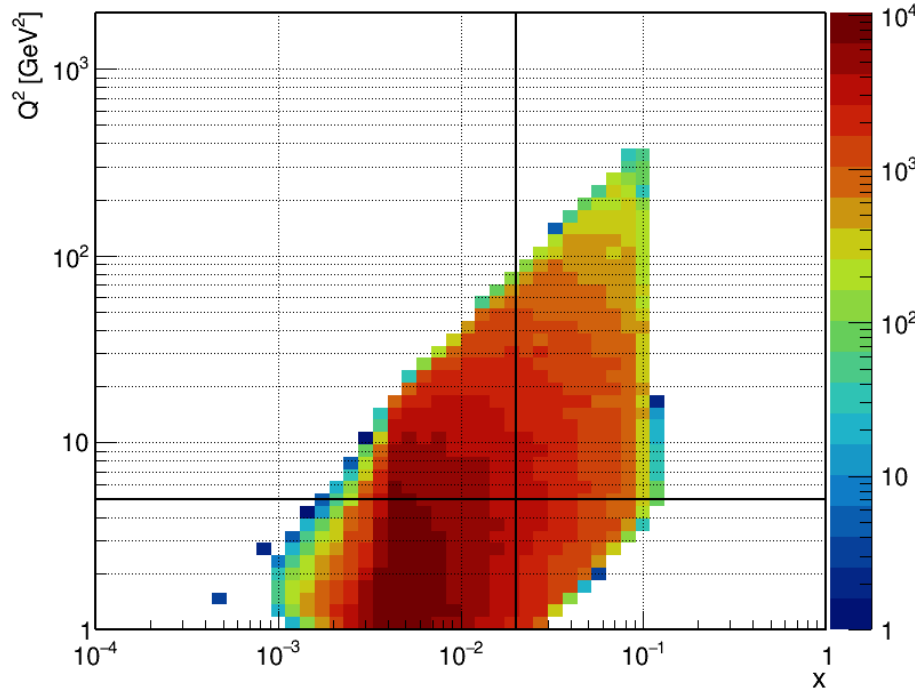


(x, Q^2) Plane for 10x100 and 18x275, and Binning for Kinematic Maps

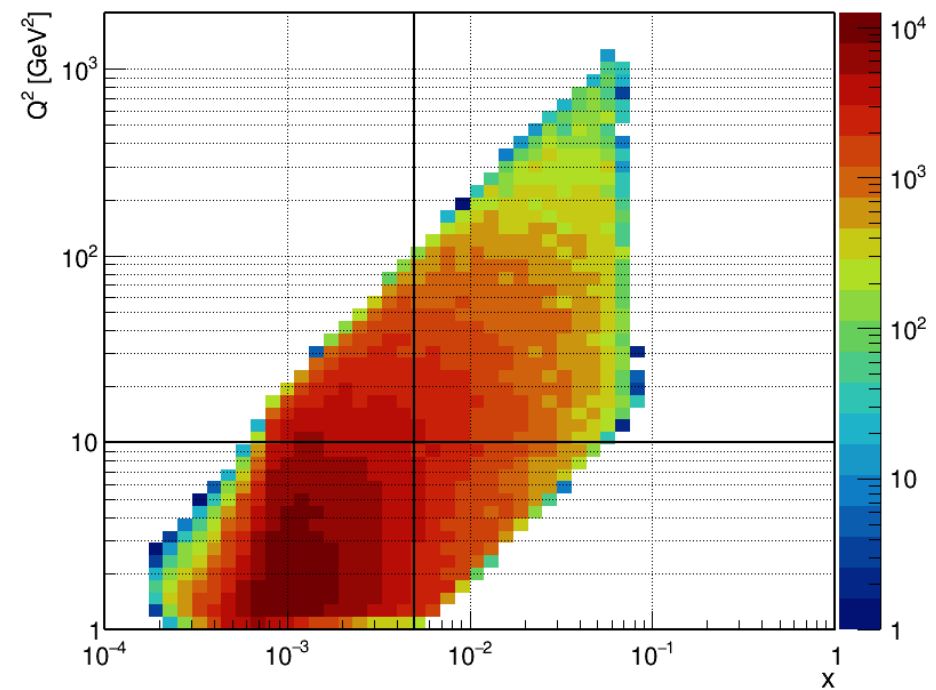
10x100 GeV

18x275 GeV

Q^2 vs. x for selected dihadrons



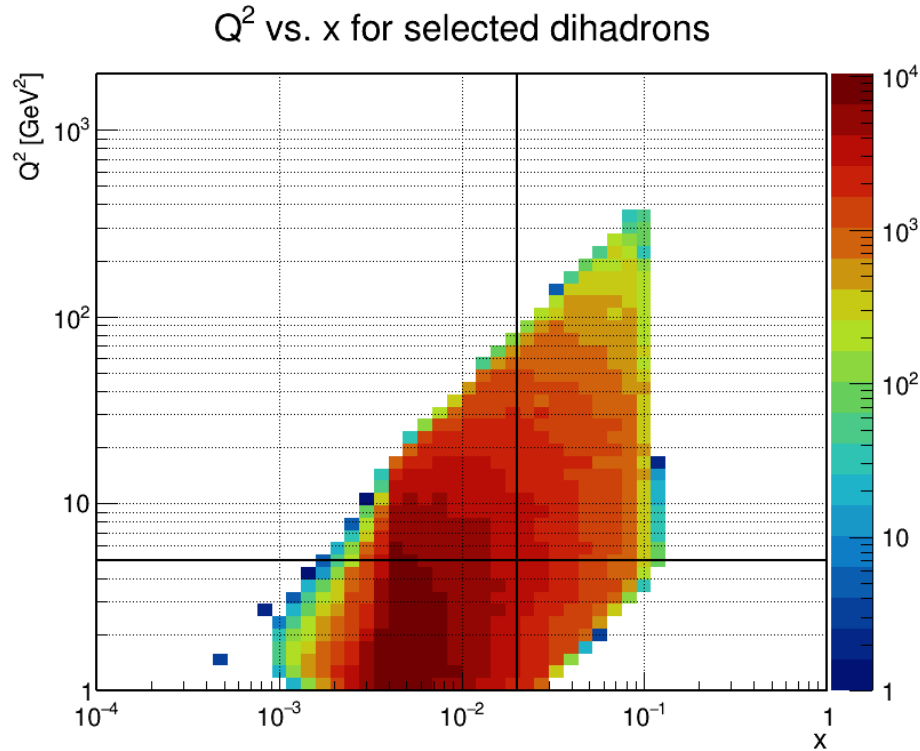
Q^2 vs. x for selected dihadrons



The next slides will focus on these two beam energy settings

Solid black lines demarcate (x, Q^2) bin boundaries, used in the following slides

(x, Q^2) Binning \rightarrow Matrix of Plots



full Q^2
range

high Q^2

low Q^2

low x

high x

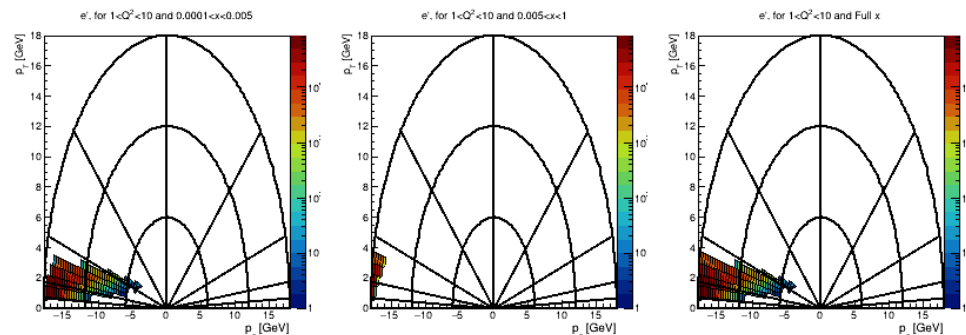
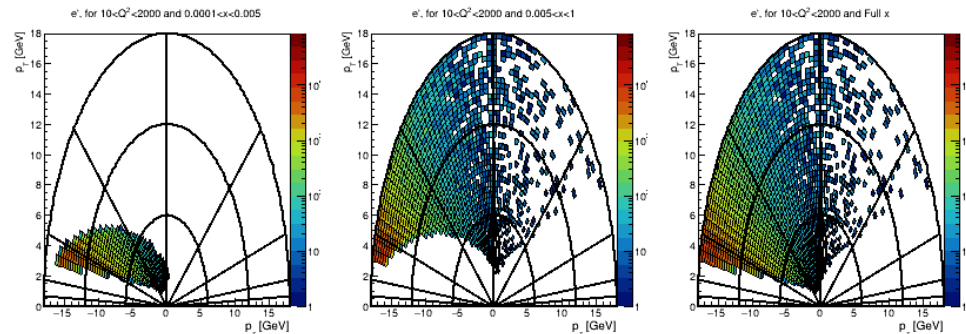
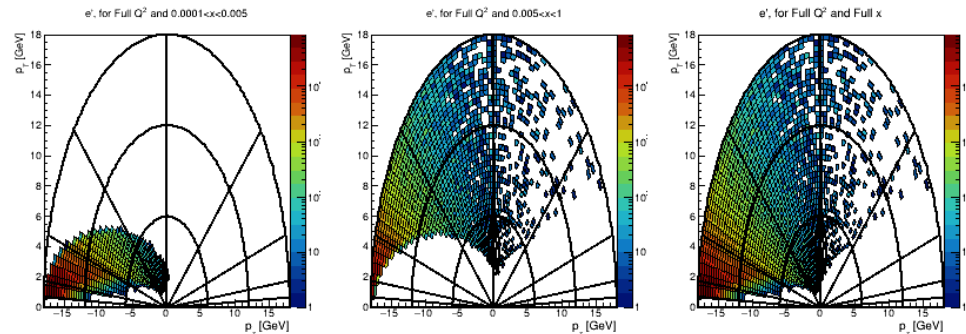
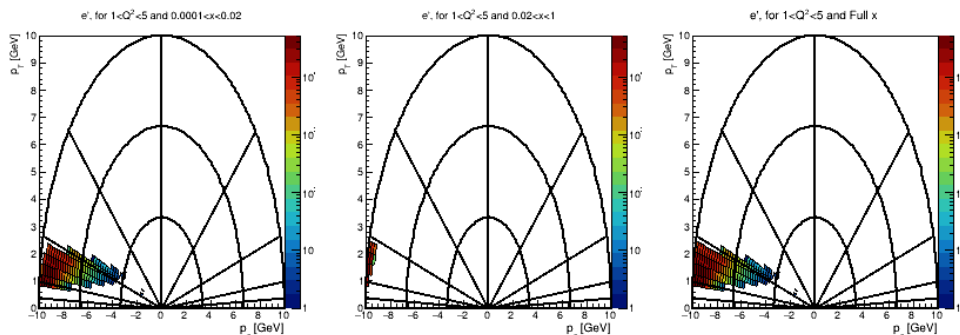
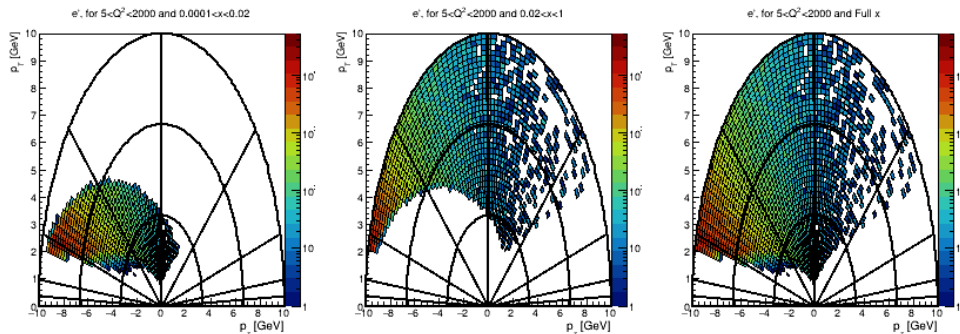
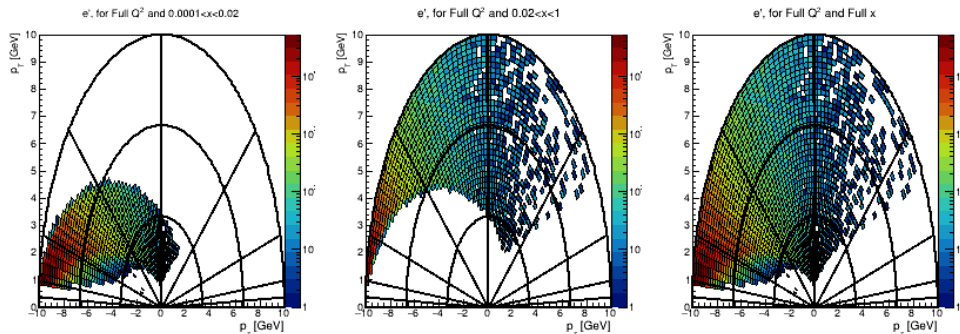
full x
range

- ▶ Bottom-left four entries are the 4 bins shown in the (x, Q^2) plane
- ▶ Top row and right row respectively integrate over Q^2 and x
- ▶ Top-right entry is for the full x and Q^2 ranges

10x100 GeV

e' p_T vs. p_z Polar Plots

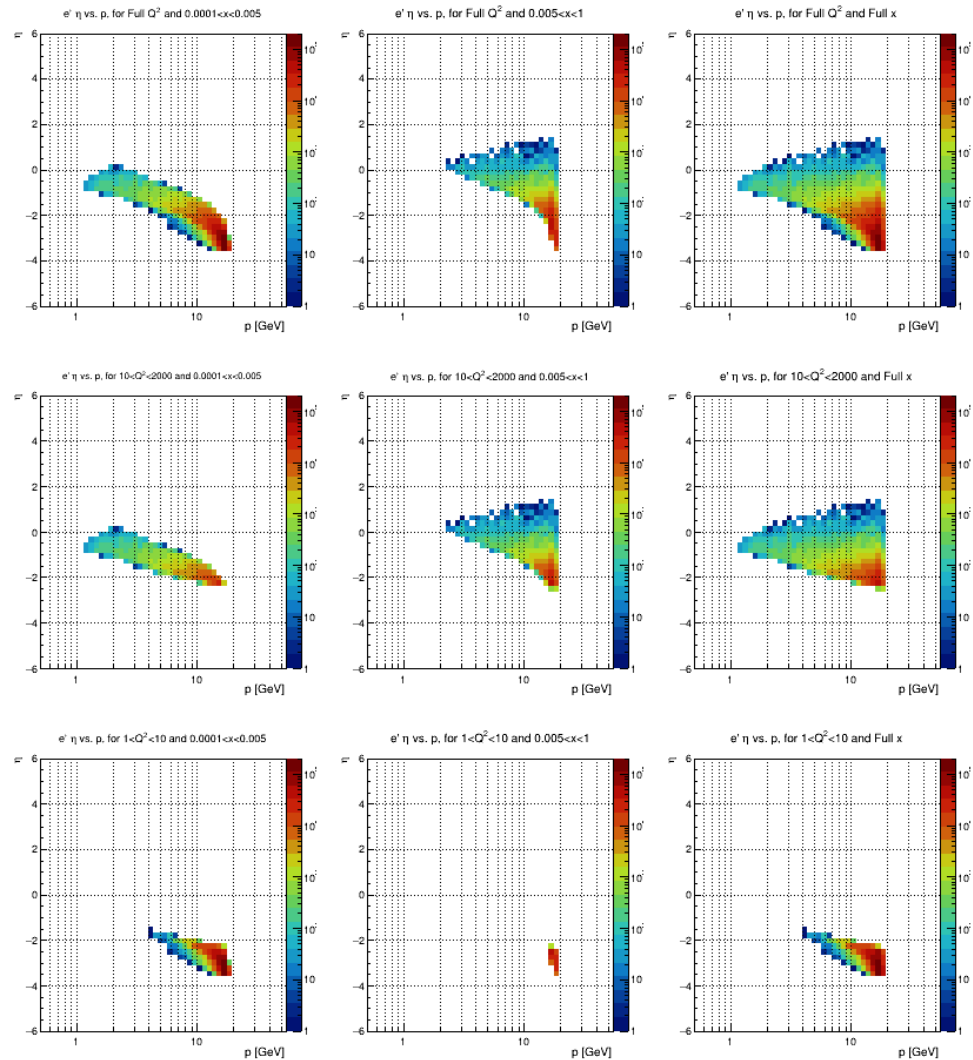
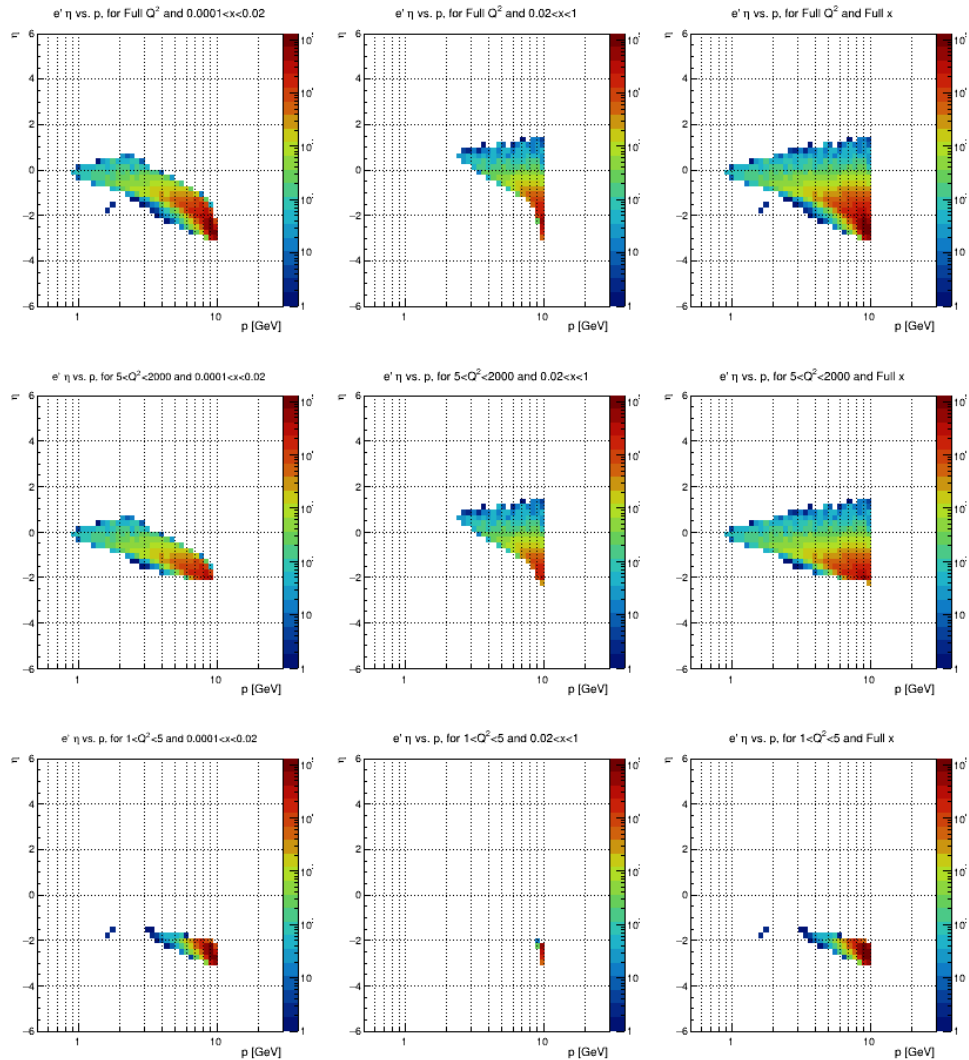
18x275 GeV



10x100 GeV

$e' \eta$ vs. p

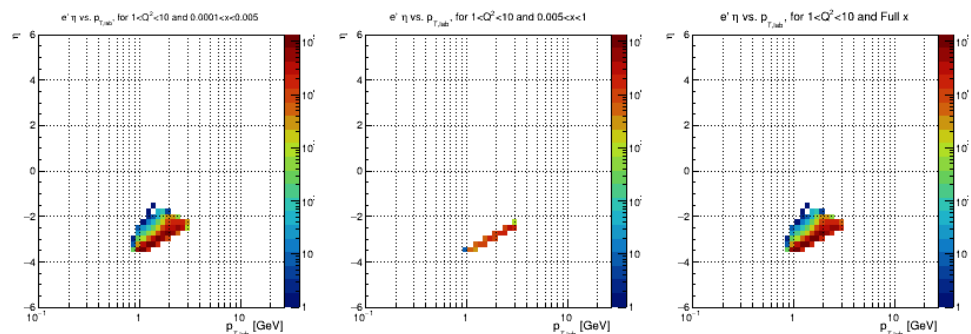
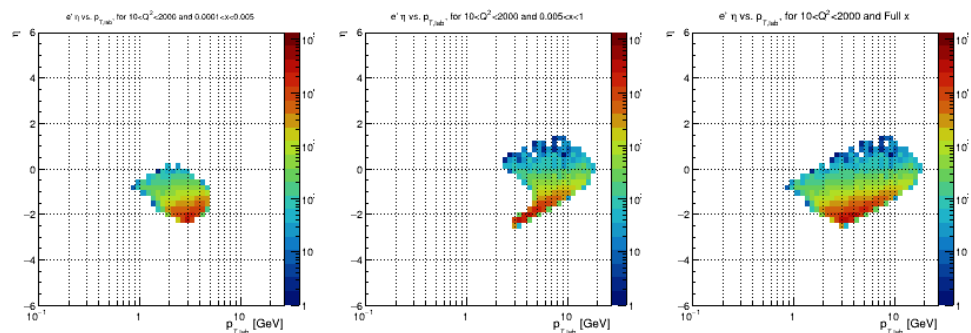
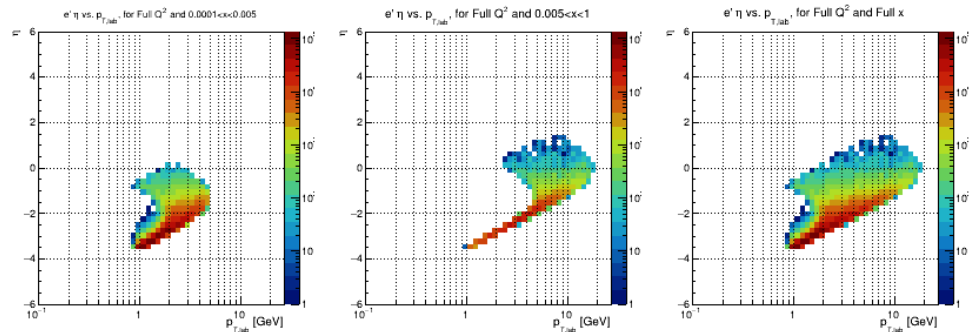
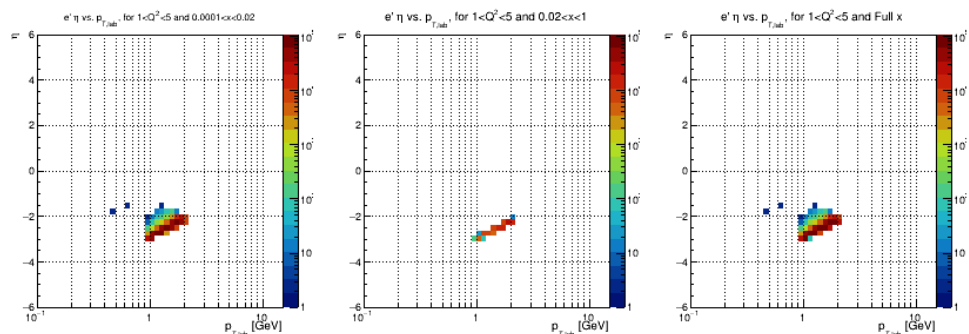
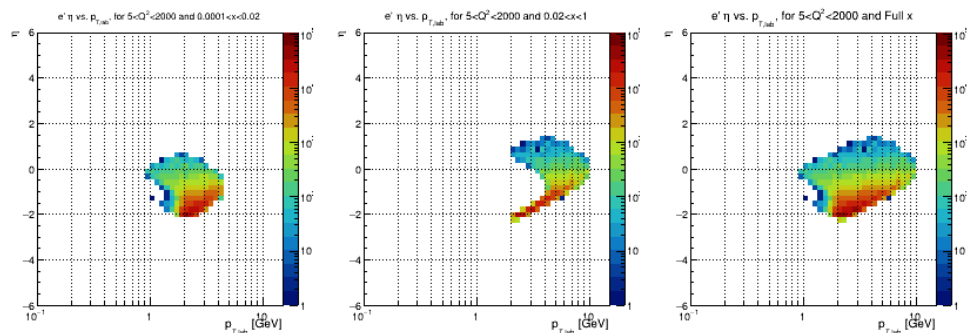
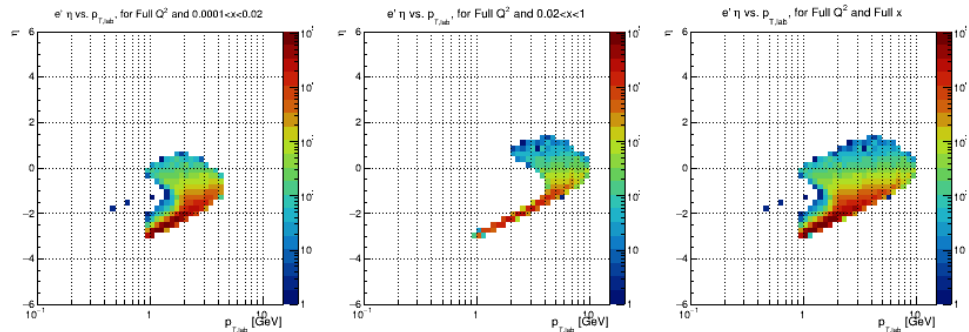
18x275 GeV



10x100 GeV

$e' \eta$ vs. $p_{T,\text{lab}}$

18x275 GeV

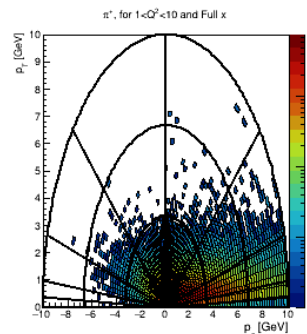
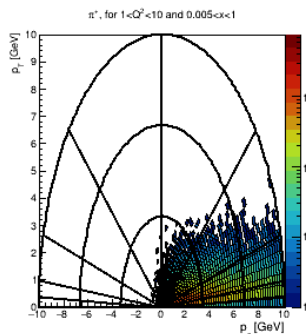
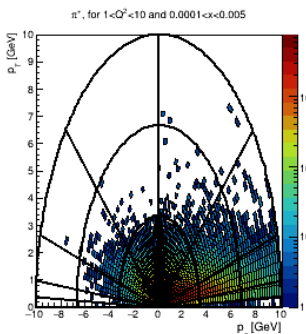
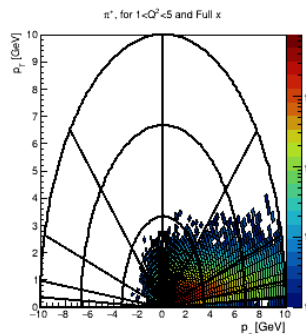
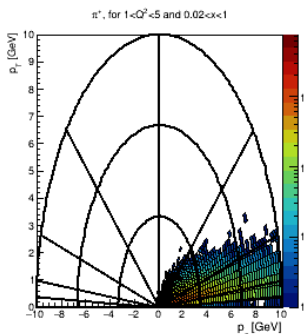
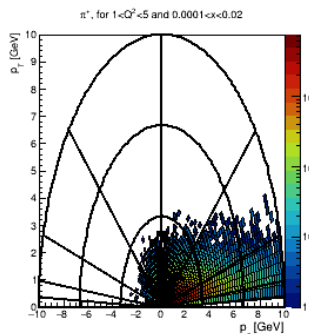
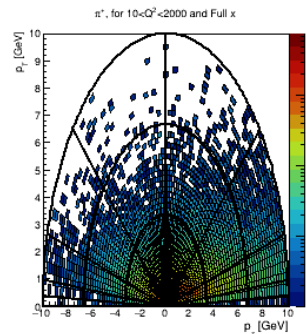
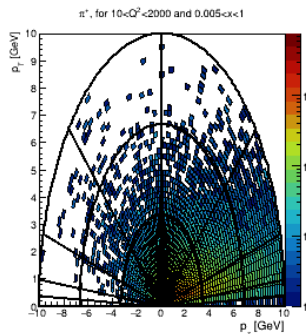
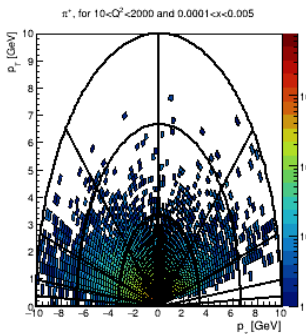
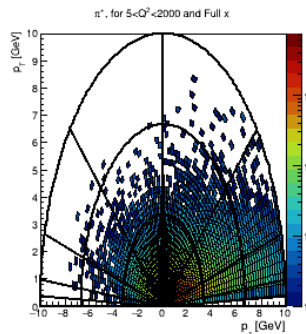
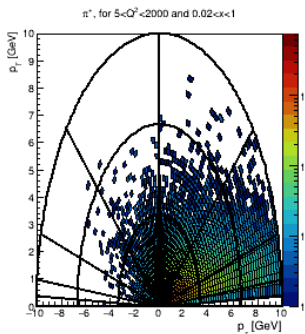
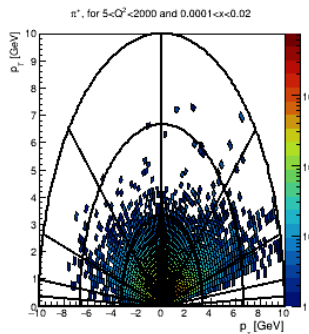
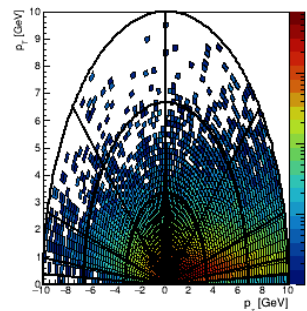
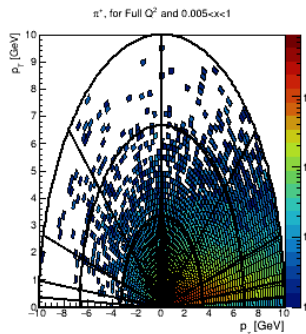
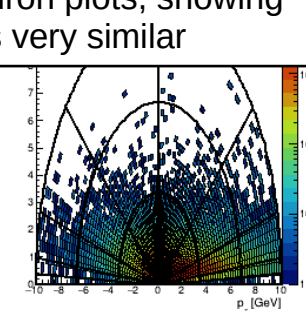
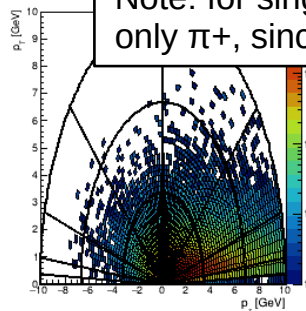
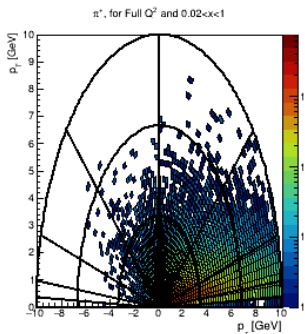
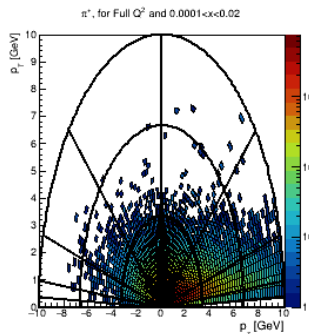


10x100 GeV

π^+ p_T vs. p_z Polar Plots

18x275 GeV

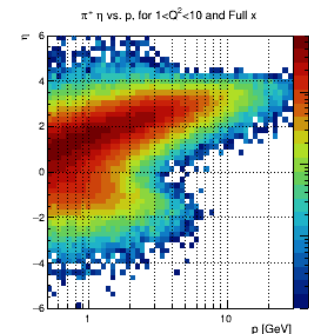
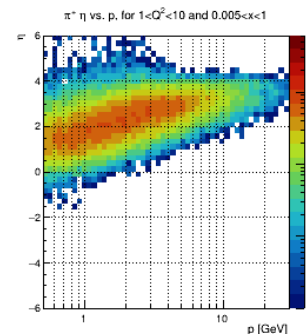
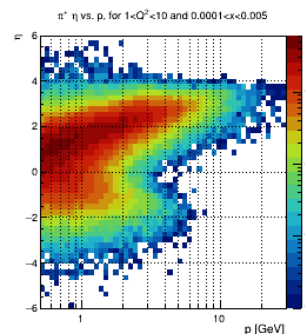
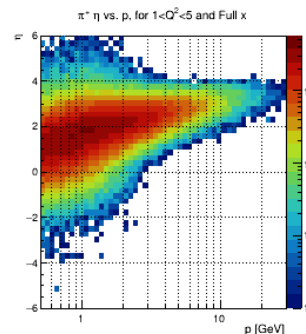
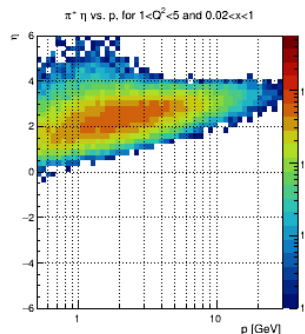
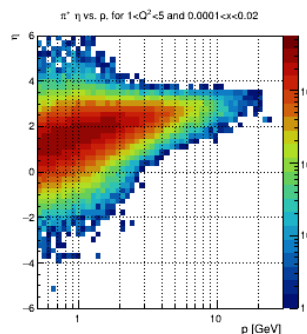
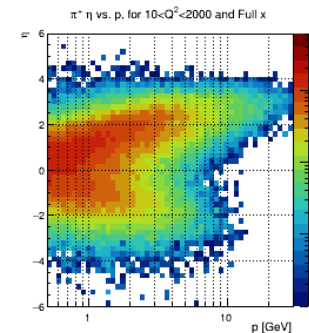
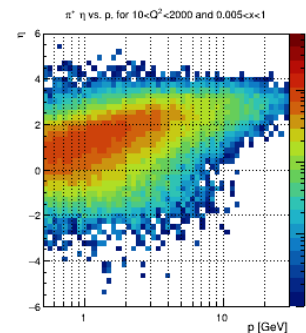
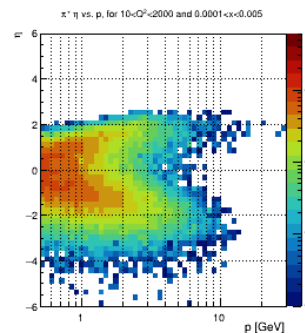
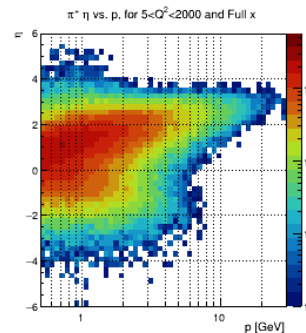
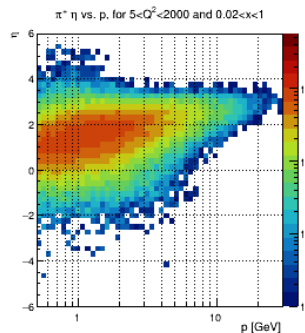
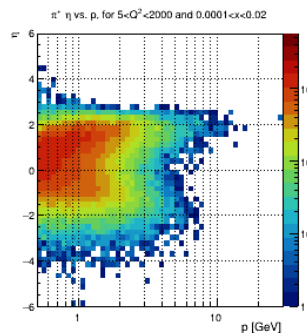
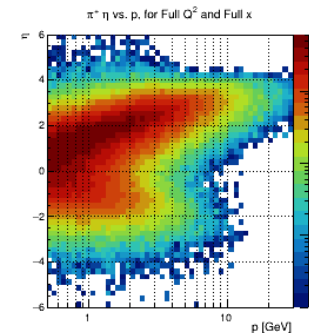
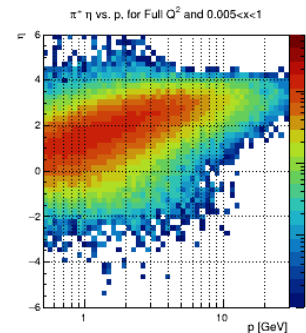
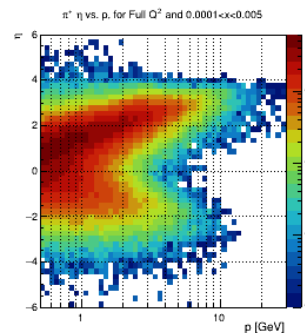
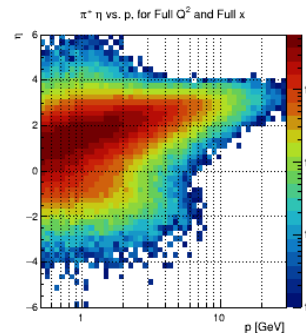
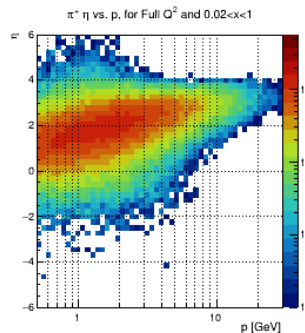
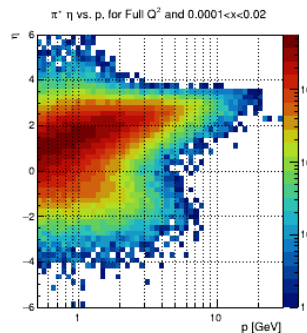
Note: for single hadron plots, showing only π^+ , since π^- is very similar



10x100 GeV

$\pi^+ \eta$ vs. p

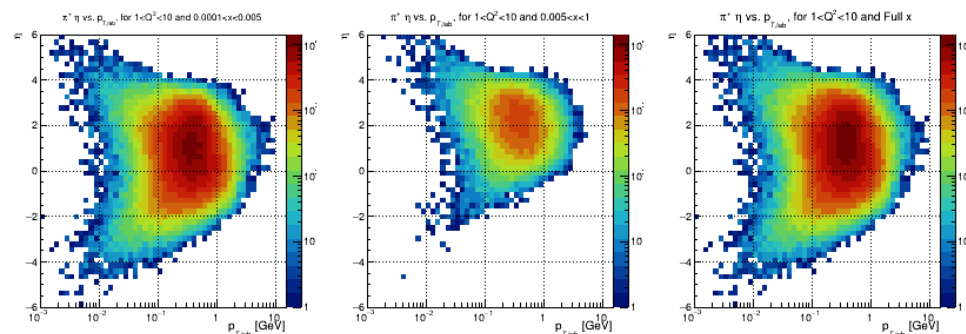
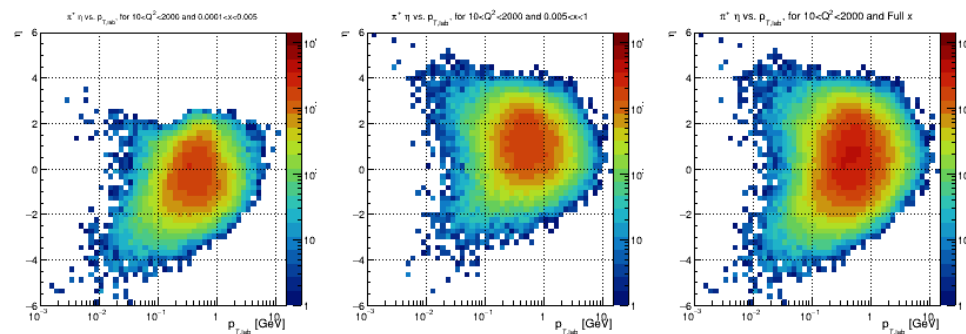
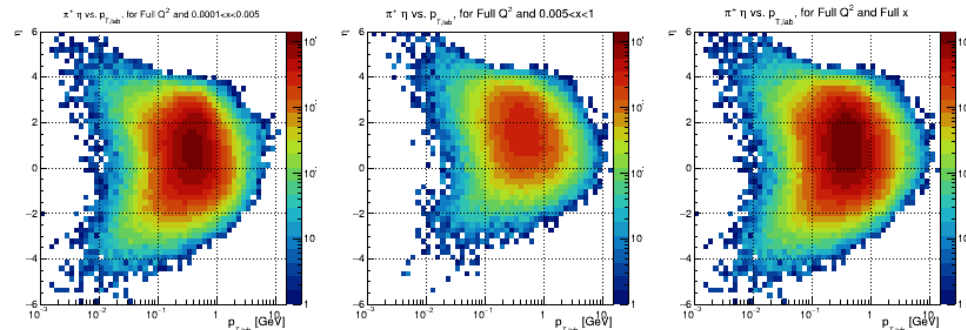
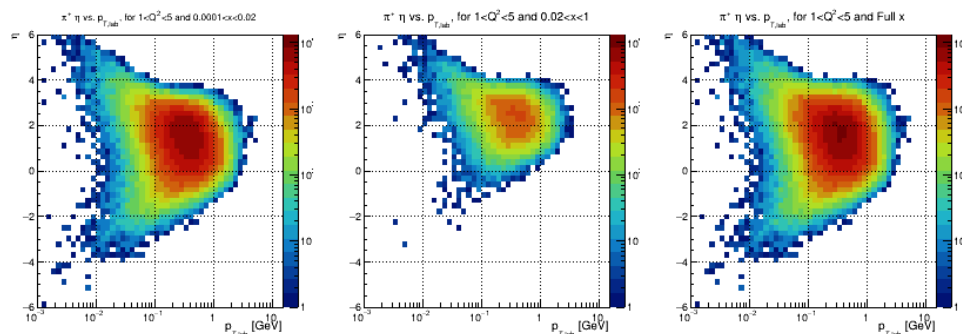
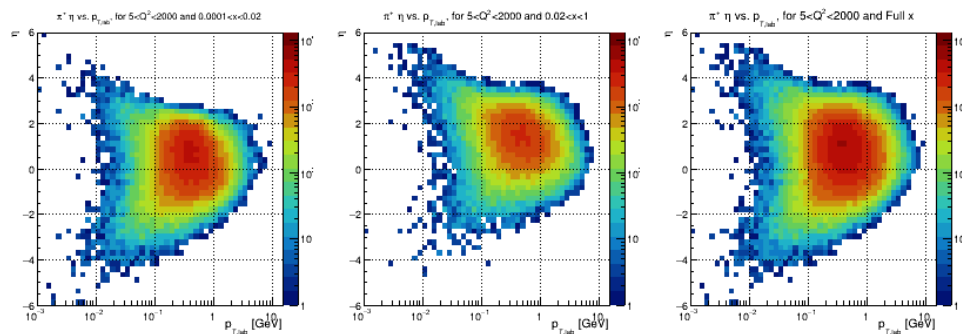
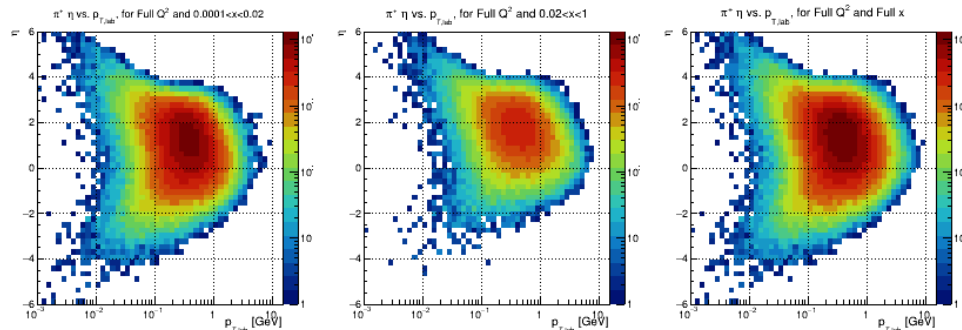
18x275 GeV



10x100 GeV

$\pi^+ \eta$ vs. $p_{T,lab}$

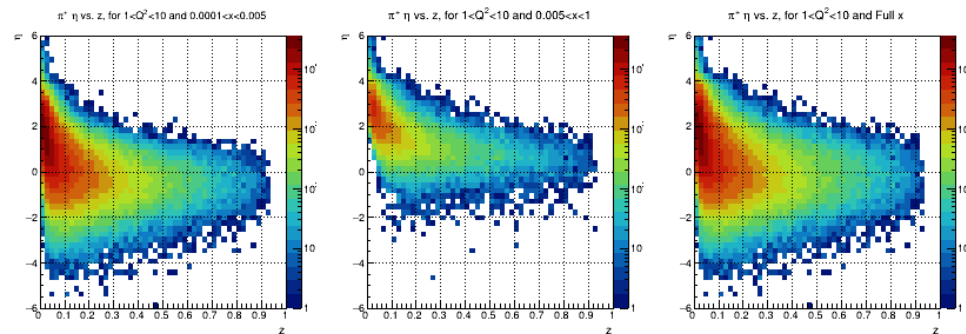
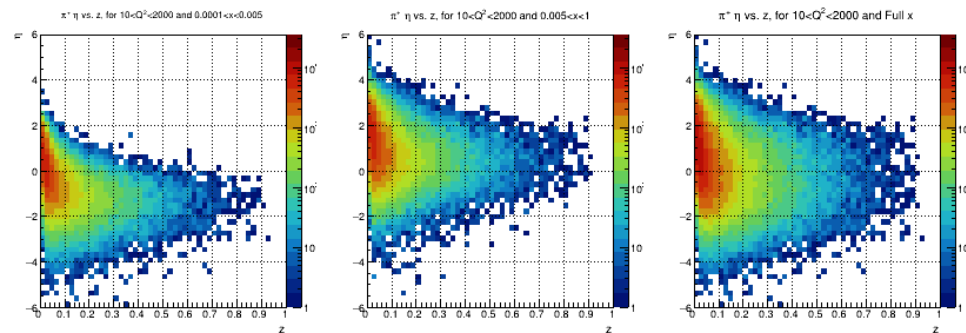
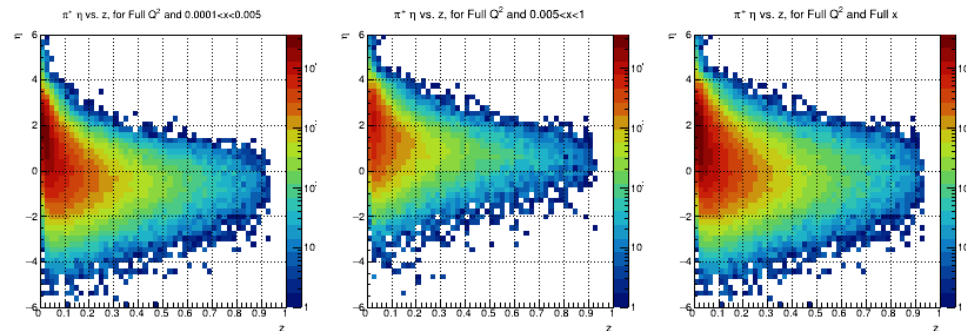
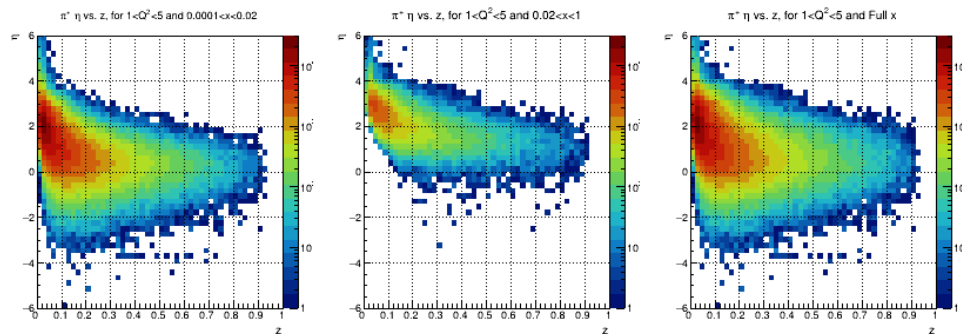
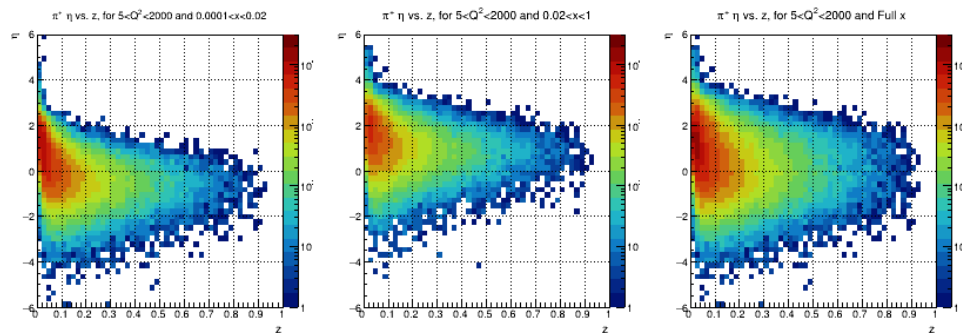
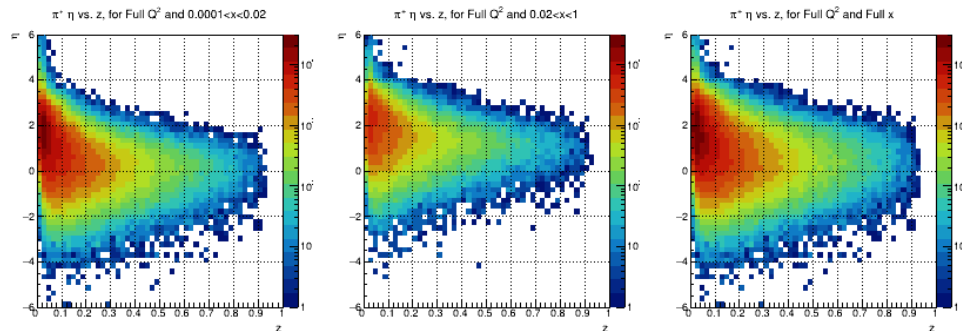
18x275 GeV



10x100 GeV

$\pi^+ \eta$ vs. z

18x275 GeV

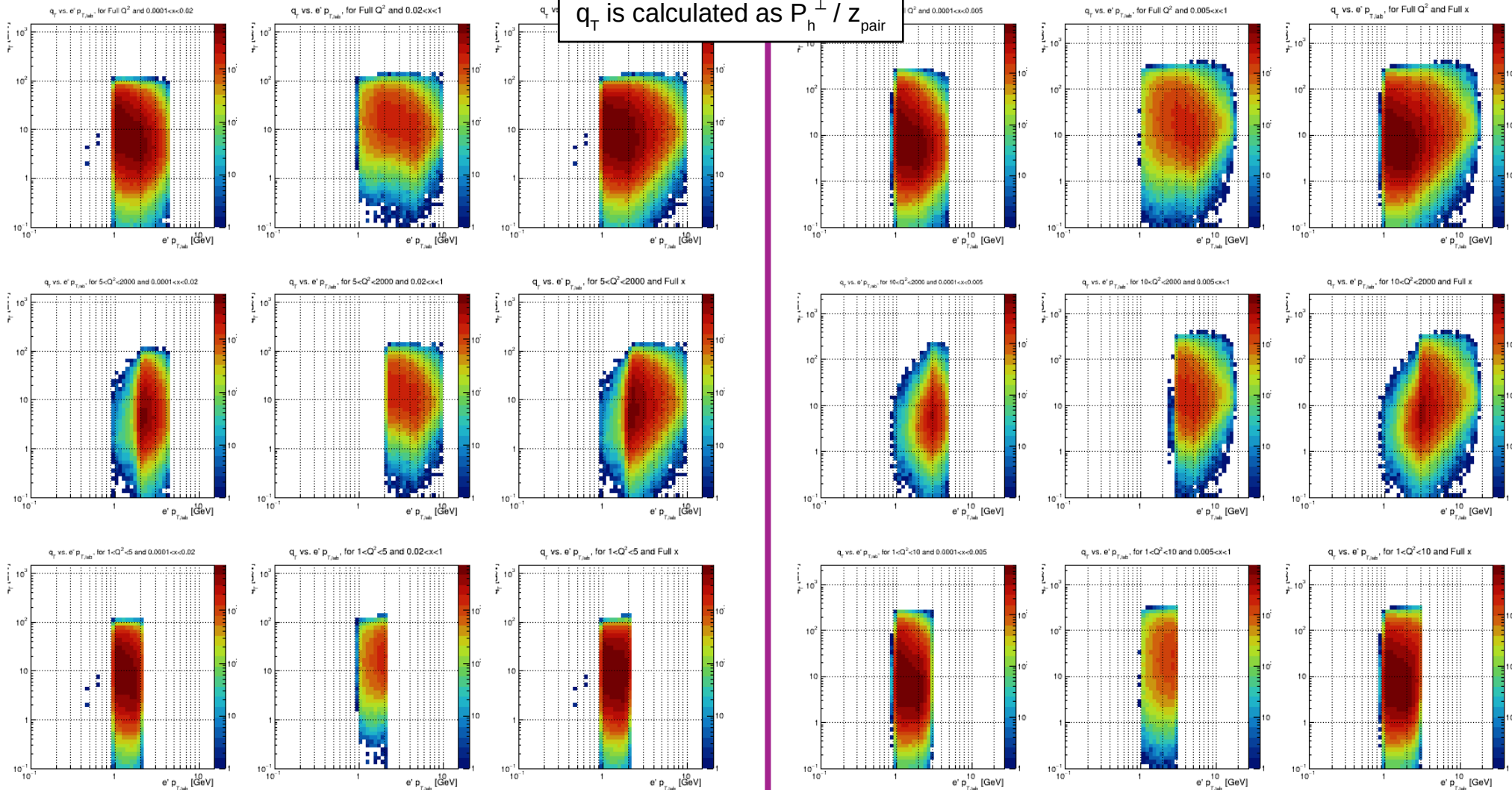


10x100 GeV

q_T vs. $e' p_{T,lab}$

18x275 GeV

q_T is calculated as P_h^\perp / z_{pair}

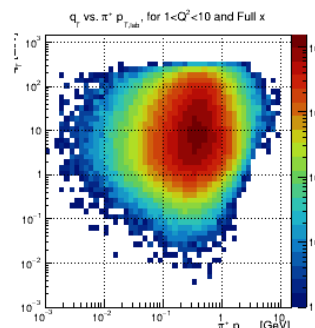
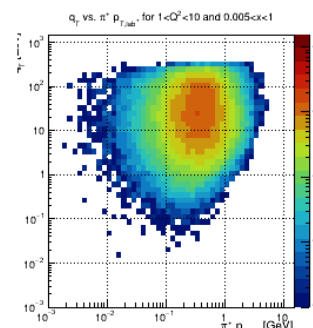
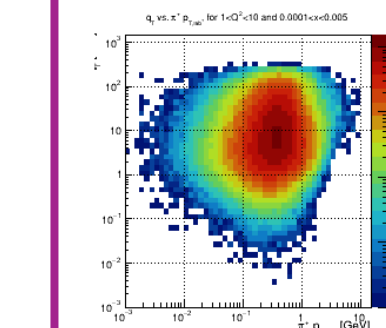
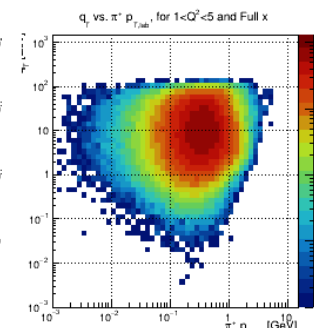
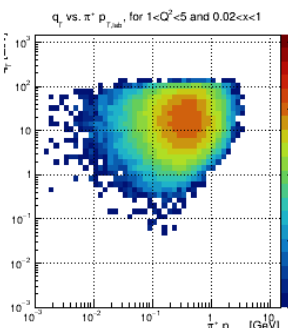
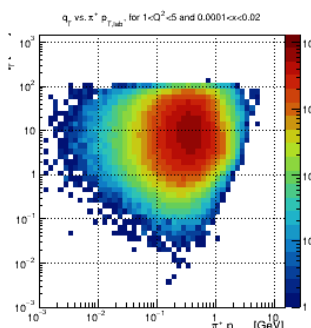
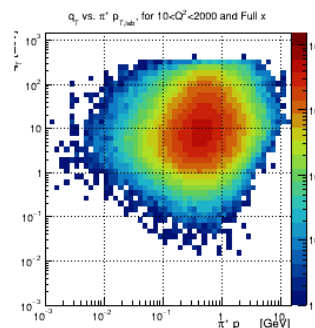
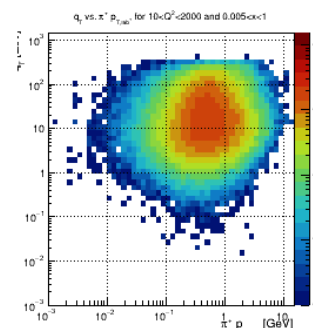
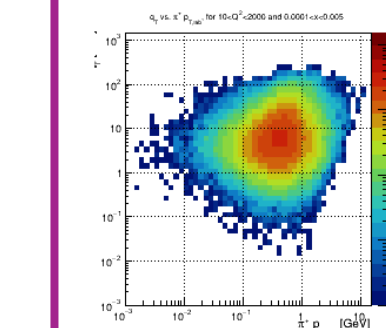
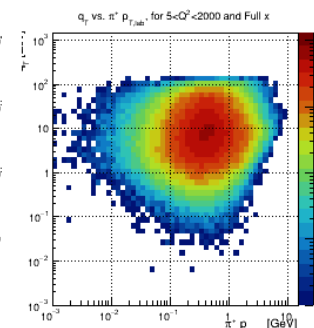
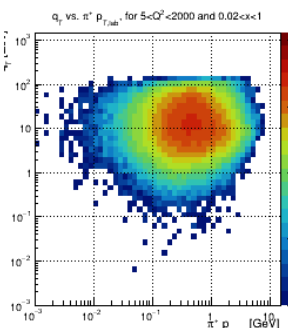
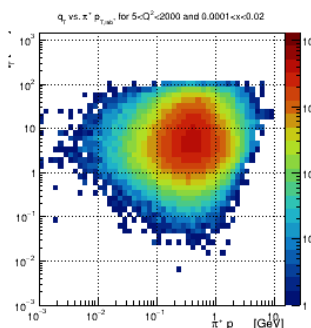
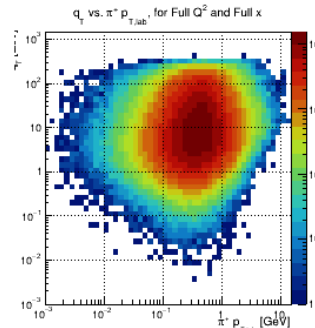
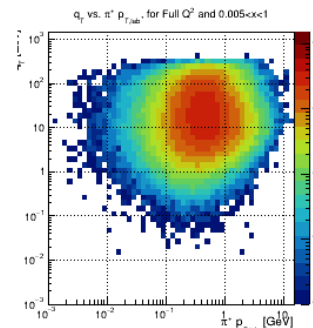
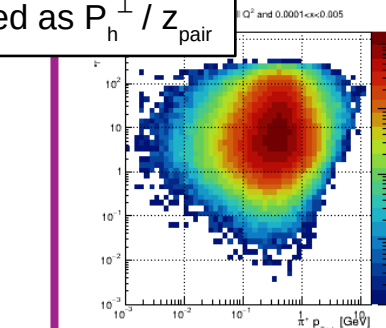
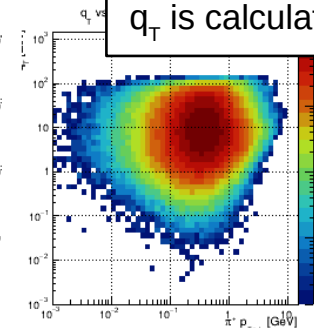
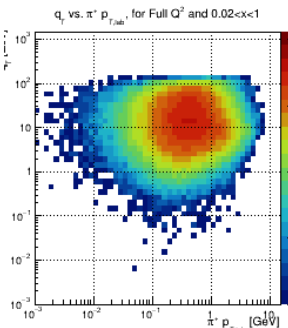
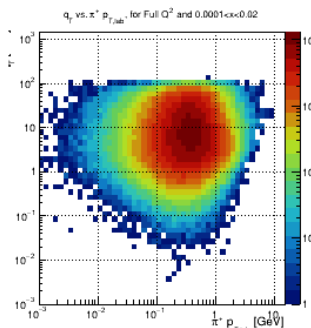


10x100 GeV

q_T vs. $\pi^+ p_T$

18x275 GeV

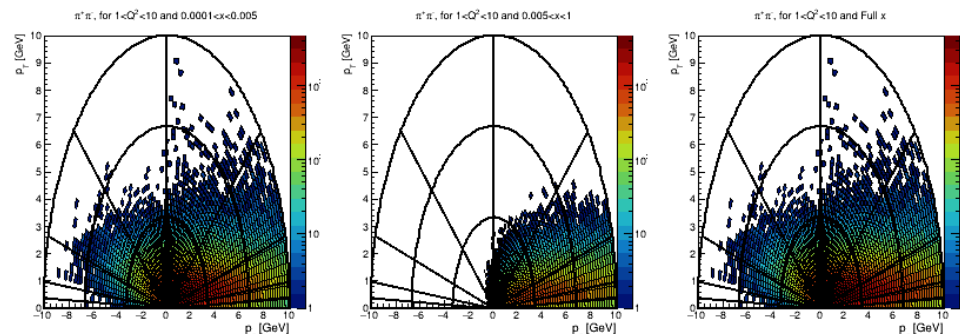
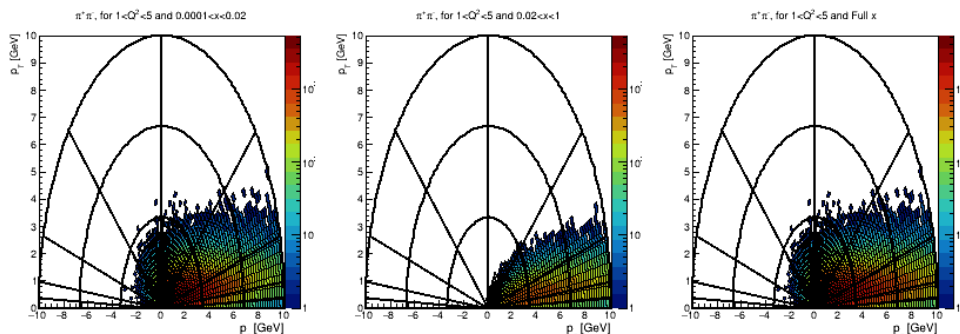
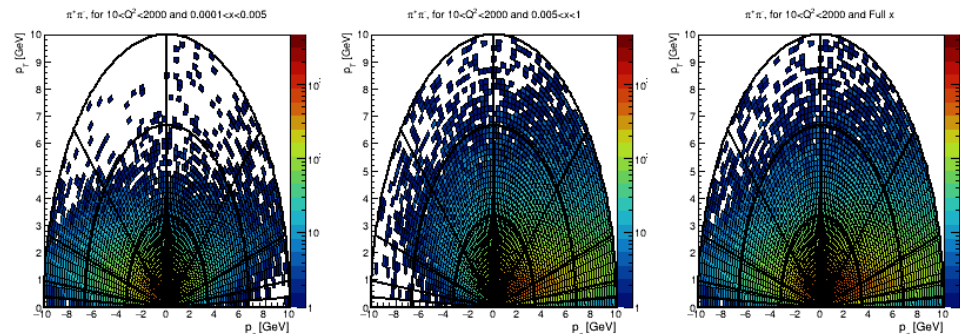
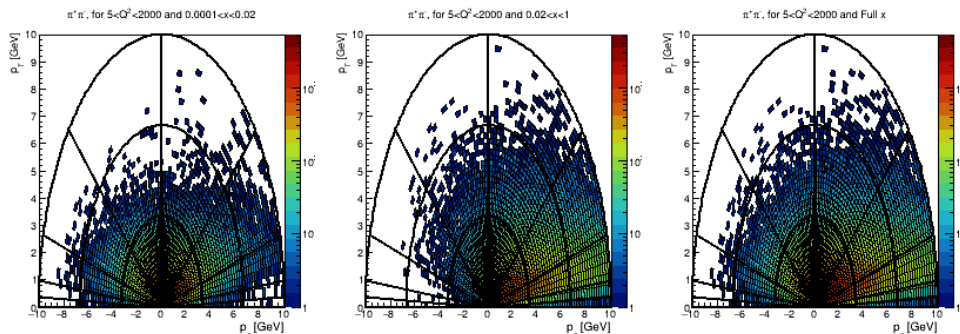
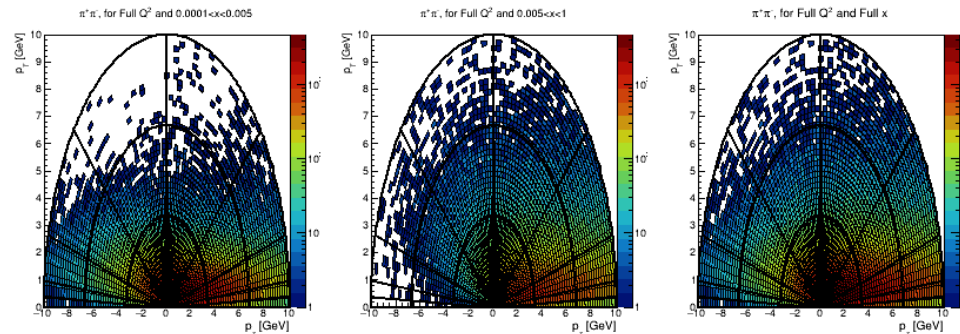
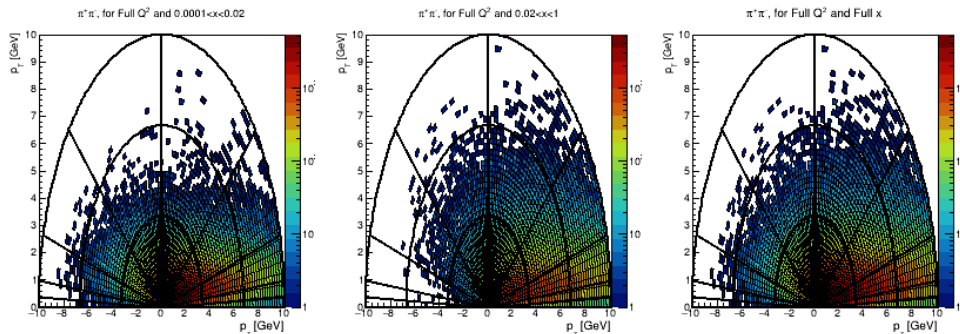
q_T is calculated as $P_h^\perp / z_{\text{pair}}$



10x100 GeV

$\pi^+\pi^-$ p_T vs. p_z Polar Plots

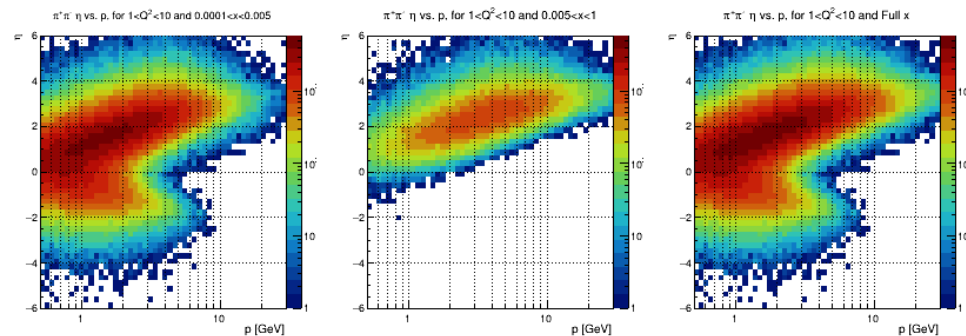
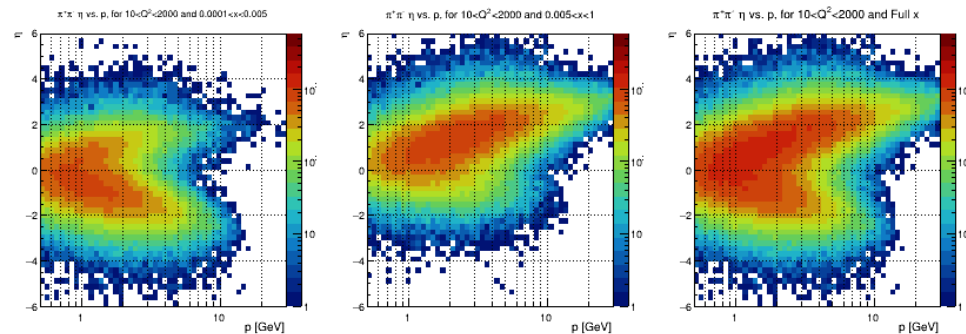
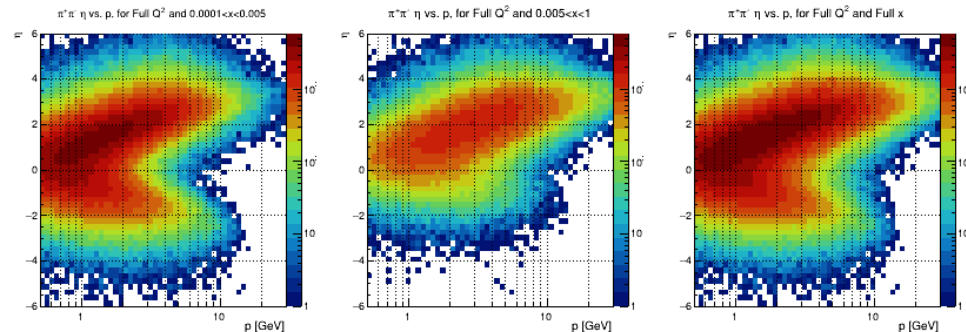
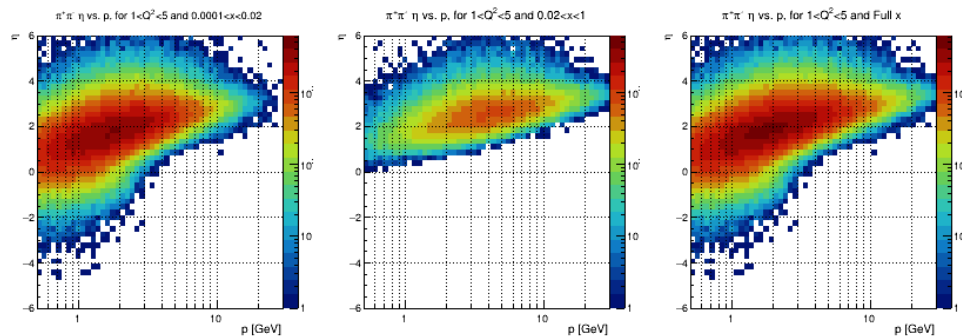
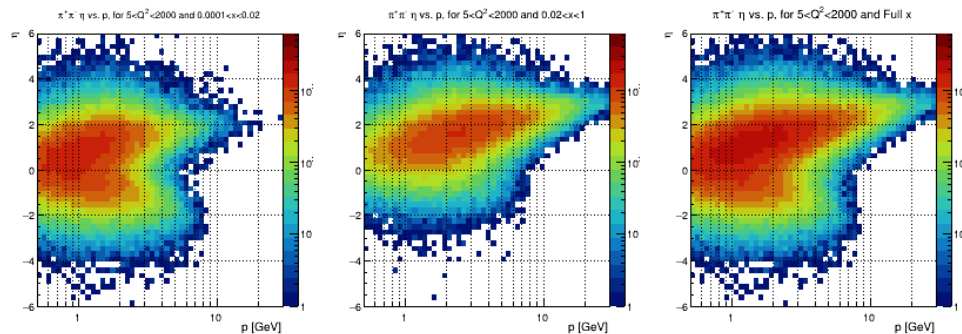
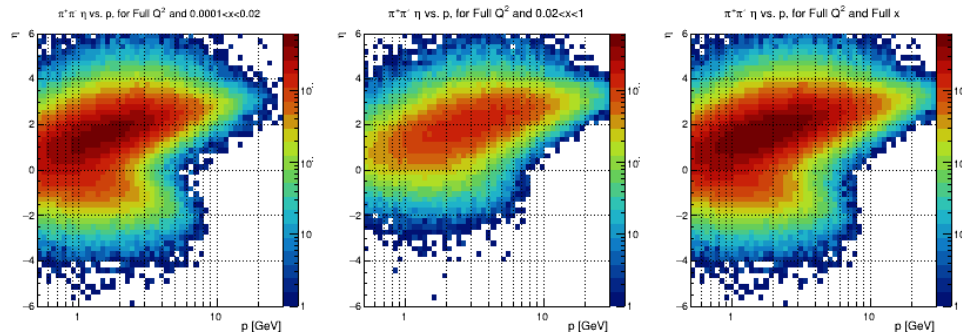
18x275 GeV



10x100 GeV

$\pi^+\pi^- \eta$ vs. p

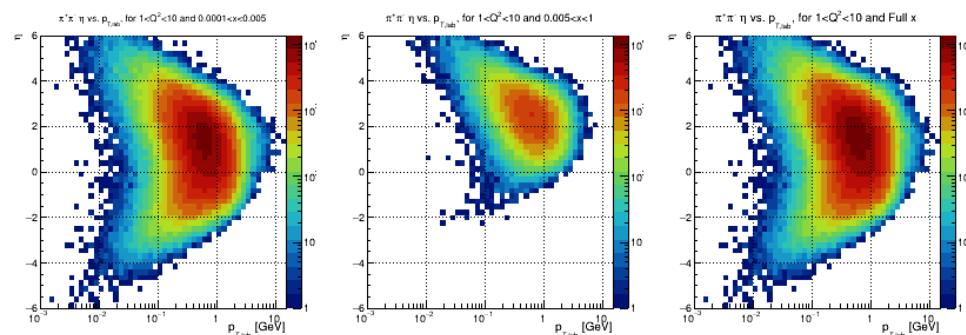
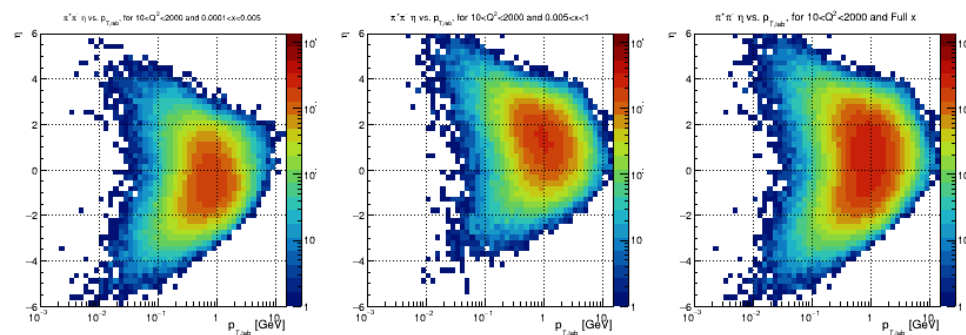
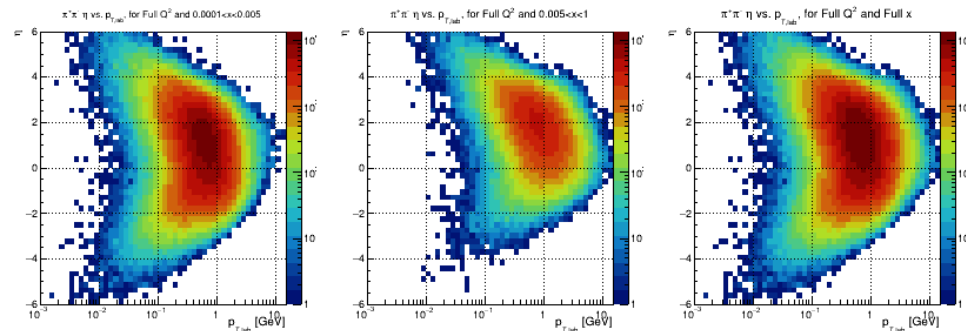
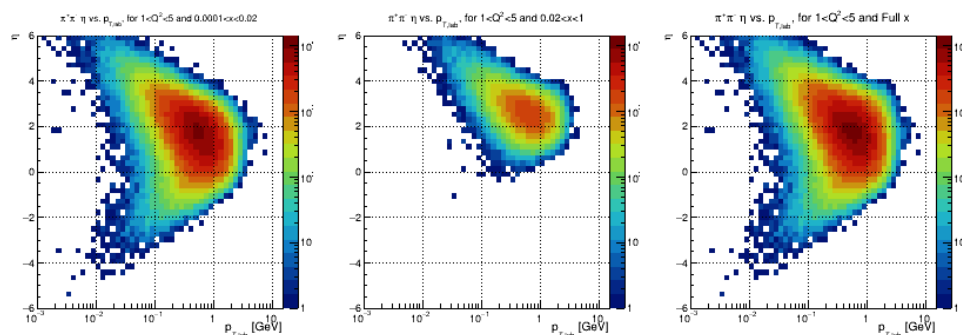
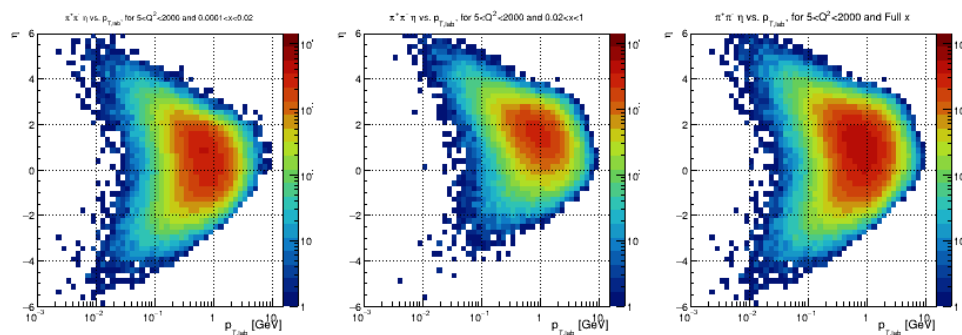
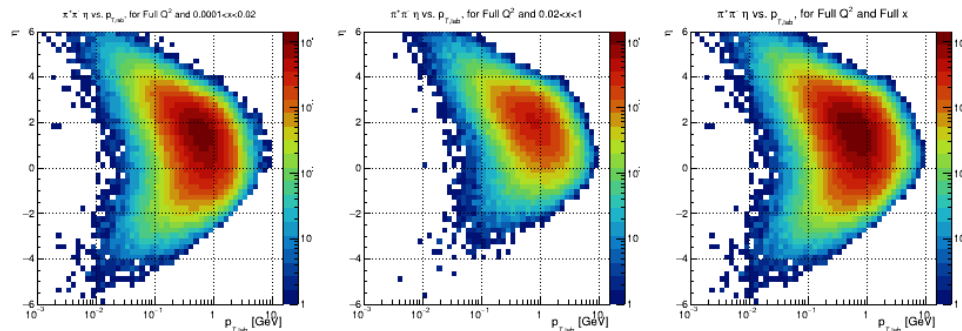
18x275 GeV



10x100 GeV

$\pi^+\pi^-\eta$ vs. p_T

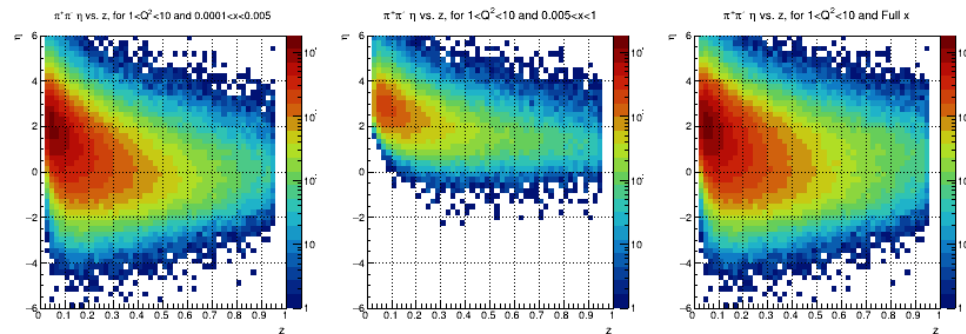
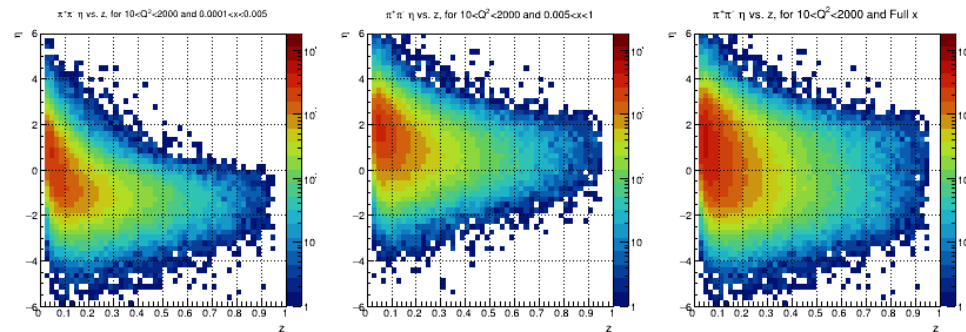
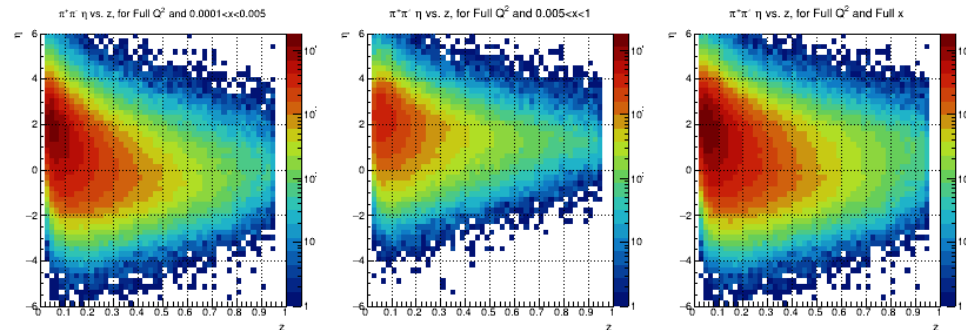
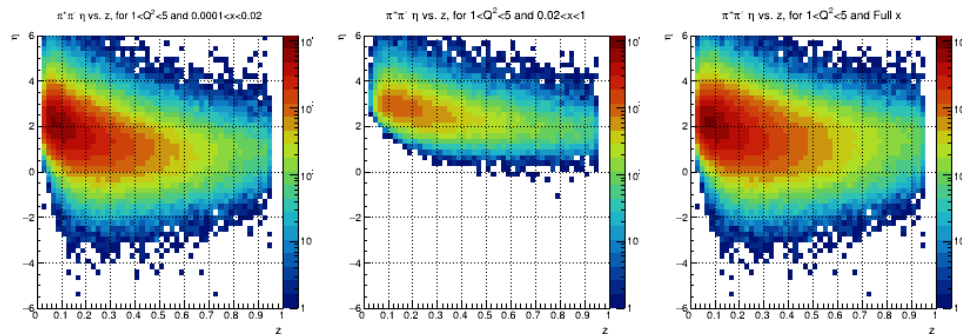
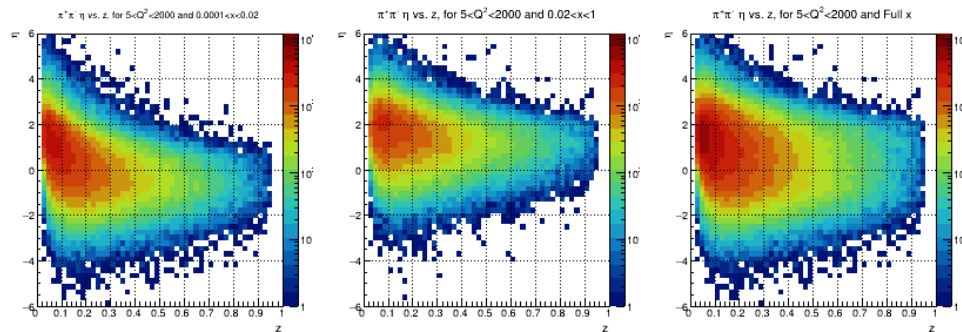
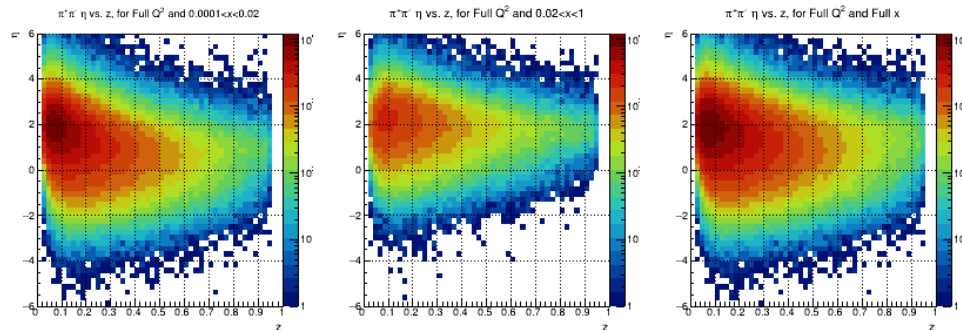
18x275 GeV



10x100 GeV

$\pi^+\pi^- \eta$ vs. z

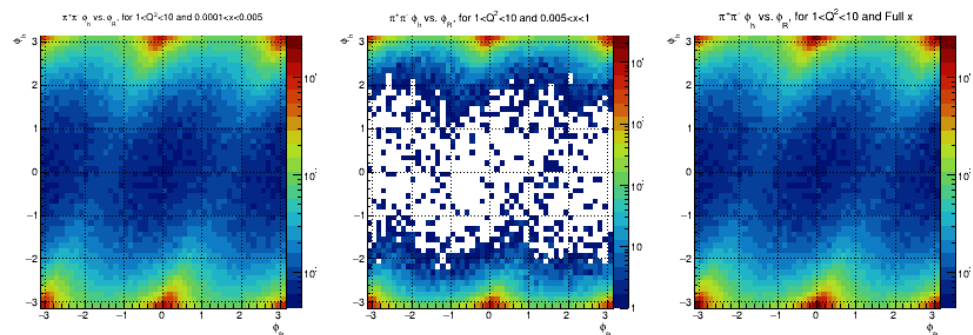
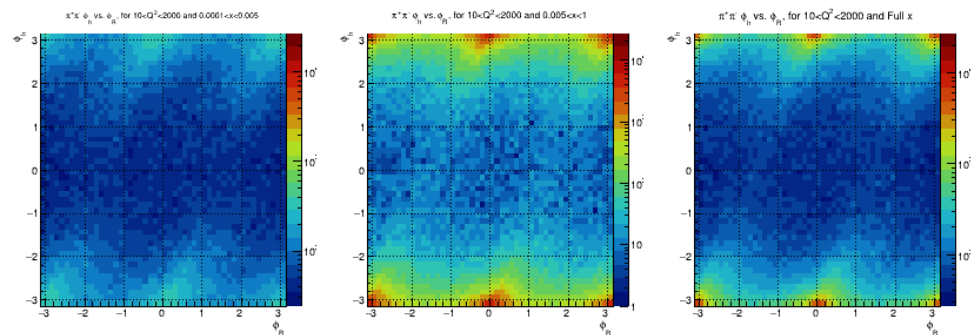
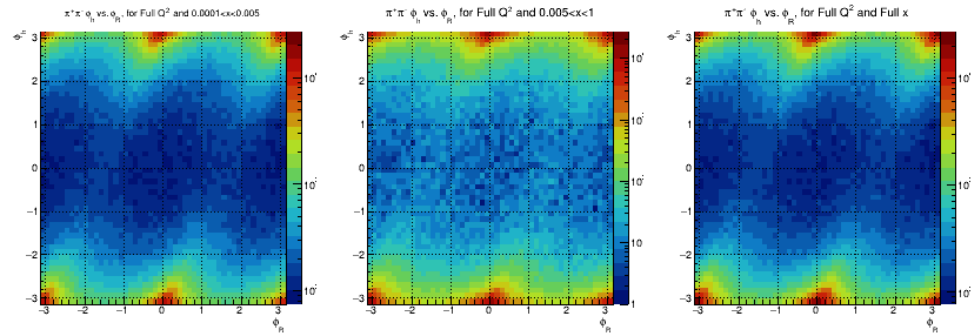
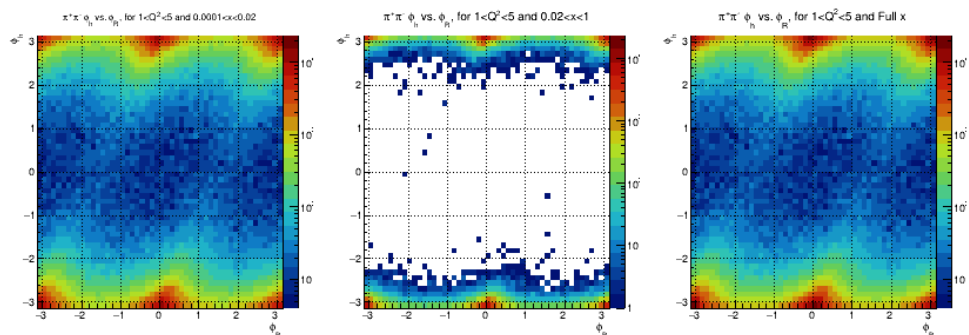
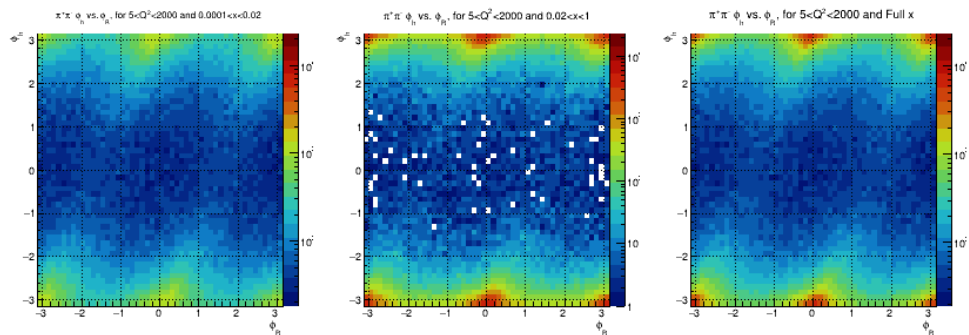
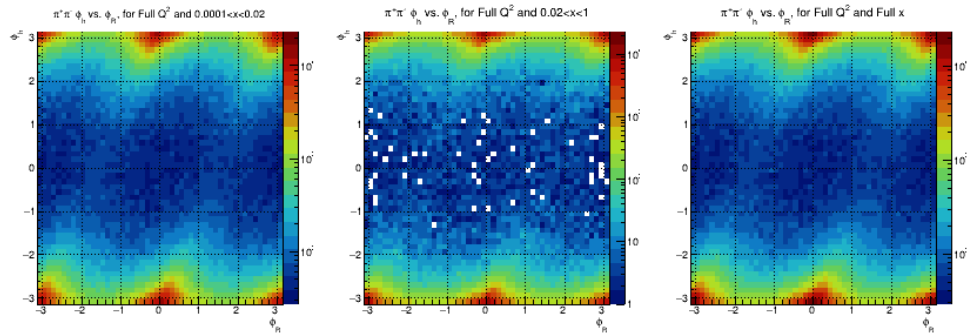
18x275 GeV



10x100 GeV

$\pi^+\pi^- \phi_h$ vs. ϕ_R

18x275 GeV

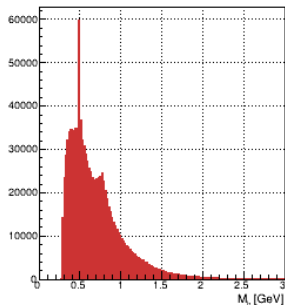


10x100 GeV

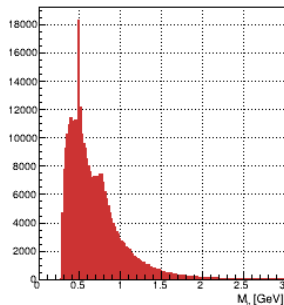
$\pi^+\pi^- M_h$ distribution

18x275 GeV

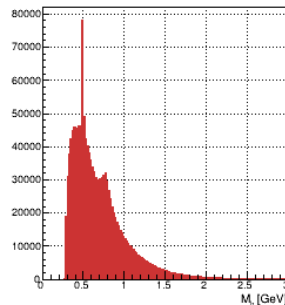
$\pi^+\pi^- M_h$ distribution, for Full Q^2 and $0.0001 < x < 0.02$



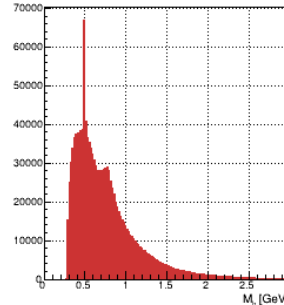
$\pi^+\pi^- M_h$ distribution, for Full Q^2 and $0.02 < x < 1$



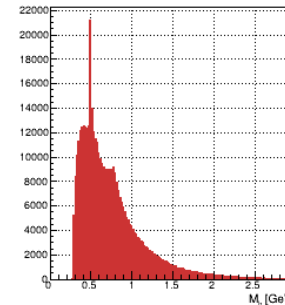
$\pi^+\pi^- M_h$ distribution, for Full Q^2 and Full x



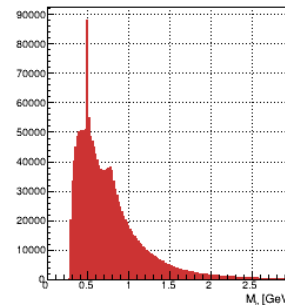
$\pi^+\pi^- M_h$ distribution, for Full Q^2 and $0.0001 < x < 0.005$



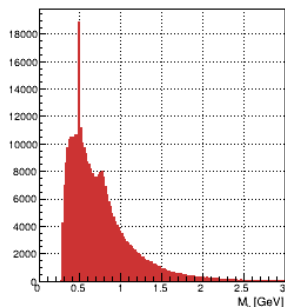
$\pi^+\pi^- M_h$ distribution, for Full Q^2 and $0.005 < x < 1$



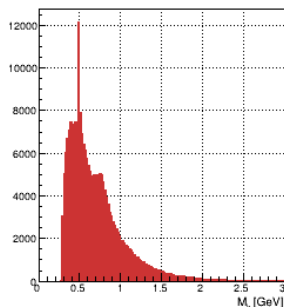
$\pi^+\pi^- M_h$ distribution, for Full Q^2 and Full x



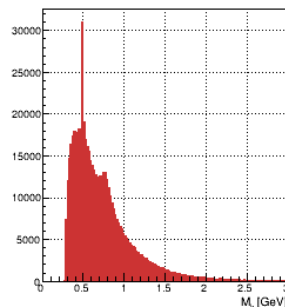
$\pi^+\pi^- M_h$ distribution, for $5 < Q^2 < 2000$ and $0.0001 < x < 0.02$



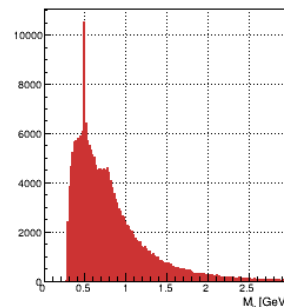
$\pi^+\pi^- M_h$ distribution, for $5 < Q^2 < 2000$ and $0.02 < x < 1$



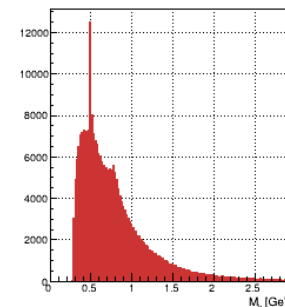
$\pi^+\pi^- M_h$ distribution, for $5 < Q^2 < 2000$ and Full x



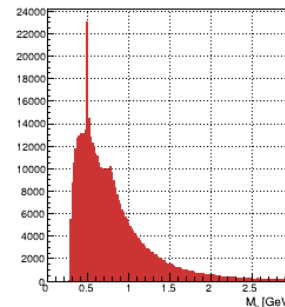
$\pi^+\pi^- M_h$ distribution, for $10 < Q^2 < 2000$ and $0.0001 < x < 0.005$



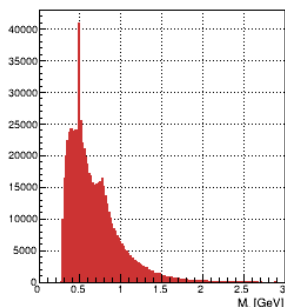
$\pi^+\pi^- M_h$ distribution, for $10 < Q^2 < 2000$ and $0.005 < x < 1$



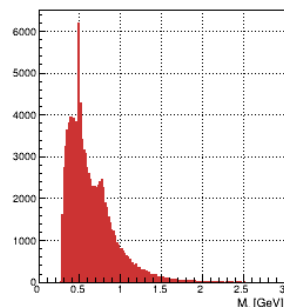
$\pi^+\pi^- M_h$ distribution, for $10 < Q^2 < 2000$ and Full x



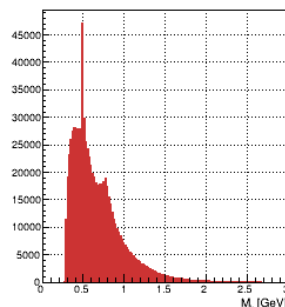
$\pi^+\pi^- M_h$ distribution, for $1 < Q^2 < 5$ and $0.0001 < x < 0.02$



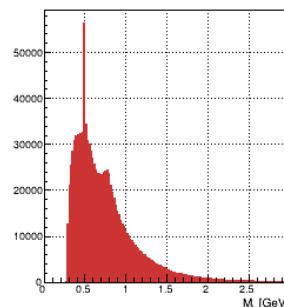
$\pi^+\pi^- M_h$ distribution, for $1 < Q^2 < 5$ and $0.02 < x < 1$



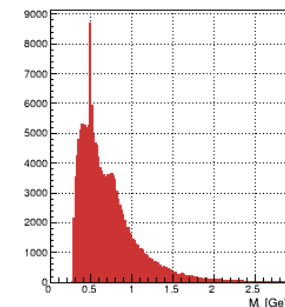
$\pi^+\pi^- M_h$ distribution, for $1 < Q^2 < 5$ and Full x



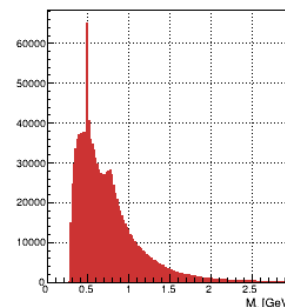
$\pi^+\pi^- M_h$ distribution, for $1 < Q^2 < 10$ and $0.0001 < x < 0.005$



$\pi^+\pi^- M_h$ distribution, for $1 < Q^2 < 10$ and $0.005 < x < 1$



$\pi^+\pi^- M_h$ distribution, for $1 < Q^2 < 10$ and Full x

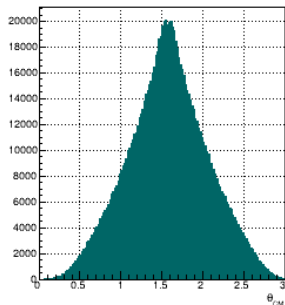


10x100 GeV

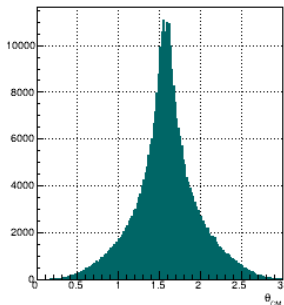
$\pi^+\pi^- \theta_{CM}$ distribution

18x275 GeV

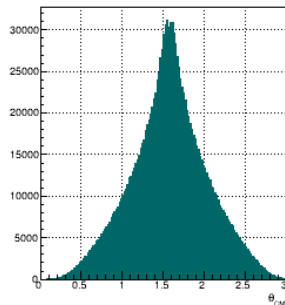
$\pi^+\pi^- \theta_{CM}$ distribution, for Full Q^2 and $0.0001 < x < 0.02$



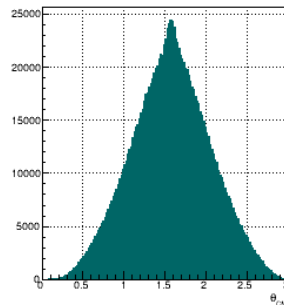
$\pi^+\pi^- \theta_{CM}$ distribution, for Full Q^2 and $0.02 < x < 1$



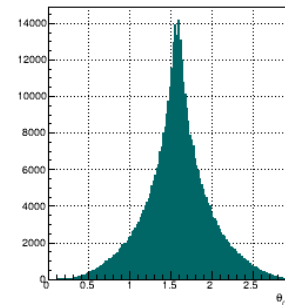
$\pi^+\pi^- \theta_{CM}$ distribution, for Full Q^2 and Full x



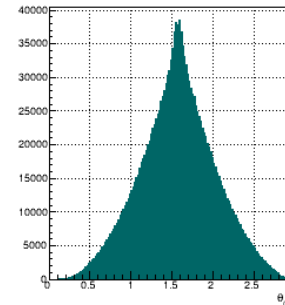
$\pi^+\pi^- \theta_{CM}$ distribution, for Full Q^2 and $0.0001 < x < 0.005$



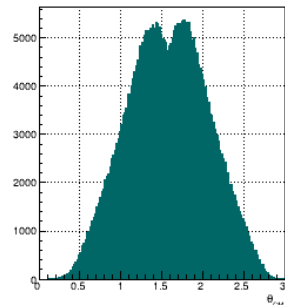
$\pi^+\pi^- \theta_{CM}$ distribution, for Full Q^2 and $0.005 < x < 1$



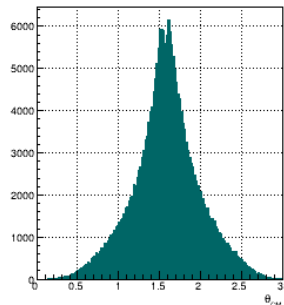
$\pi^+\pi^- \theta_{CM}$ distribution, for Full Q^2 and Full x



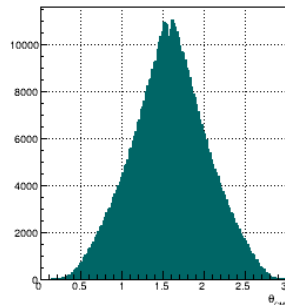
$\pi^+\pi^- \theta_{CM}$ distribution, for $5 < Q^2 < 2000$ and $0.0001 < x < 0.02$



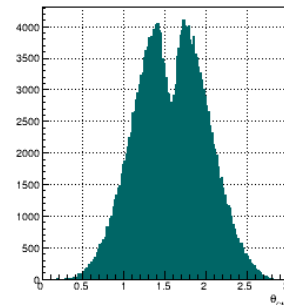
$\pi^+\pi^- \theta_{CM}$ distribution, for $5 < Q^2 < 2000$ and $0.02 < x < 1$



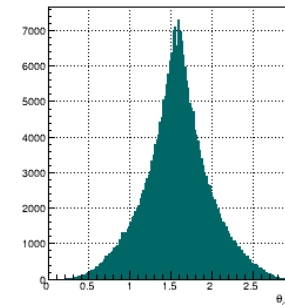
$\pi^+\pi^- \theta_{CM}$ distribution, for $5 < Q^2 < 2000$ and Full x



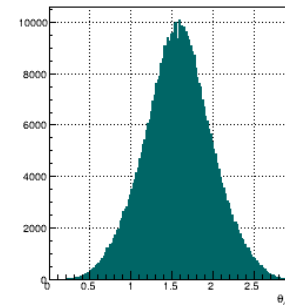
$\pi^+\pi^- \theta_{CM}$ distribution, for $10 < Q^2 < 2000$ and $0.0001 < x < 0.005$



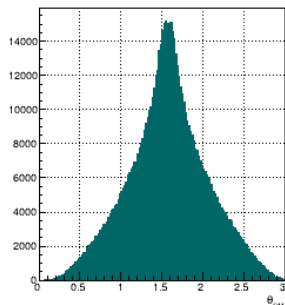
$\pi^+\pi^- \theta_{CM}$ distribution, for $10 < Q^2 < 2000$ and $0.005 < x < 1$



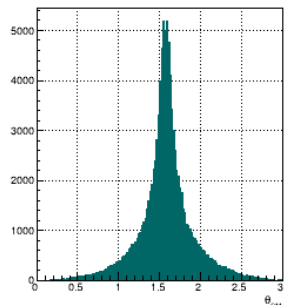
$\pi^+\pi^- \theta_{CM}$ distribution, for $10 < Q^2 < 2000$ and Full x



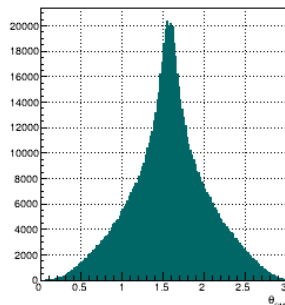
$\pi^+\pi^- \theta_{CM}$ distribution, for $1 < Q^2 < 5$ and $0.0001 < x < 0.02$



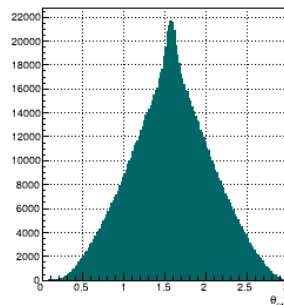
$\pi^+\pi^- \theta_{CM}$ distribution, for $1 < Q^2 < 5$ and $0.02 < x < 1$



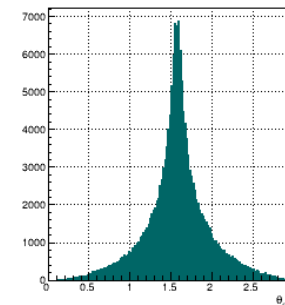
$\pi^+\pi^- \theta_{CM}$ distribution, for $1 < Q^2 < 5$ and Full x



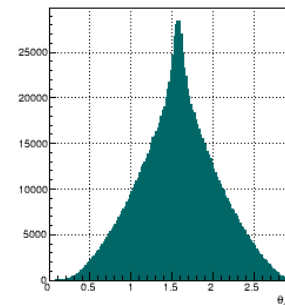
$\pi^+\pi^- \theta_{CM}$ distribution, for $1 < Q^2 < 10$ and $0.0001 < x < 0.005$



$\pi^+\pi^- \theta_{CM}$ distribution, for $1 < Q^2 < 10$ and $0.005 < x < 1$



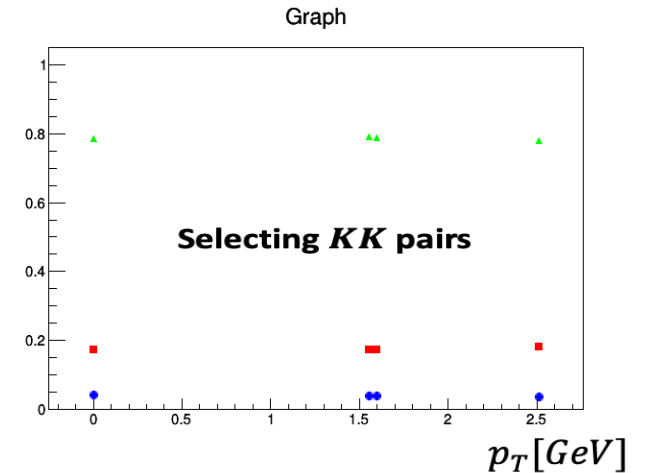
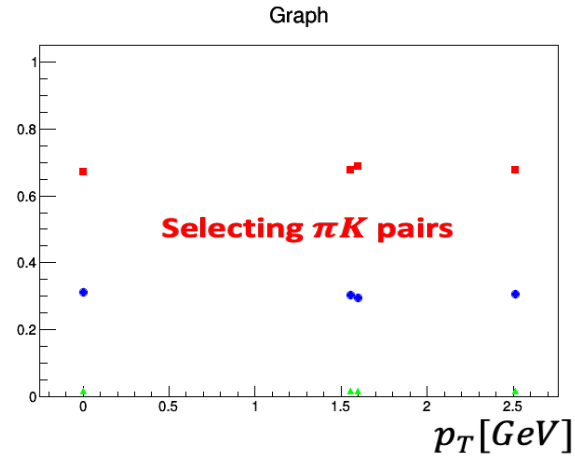
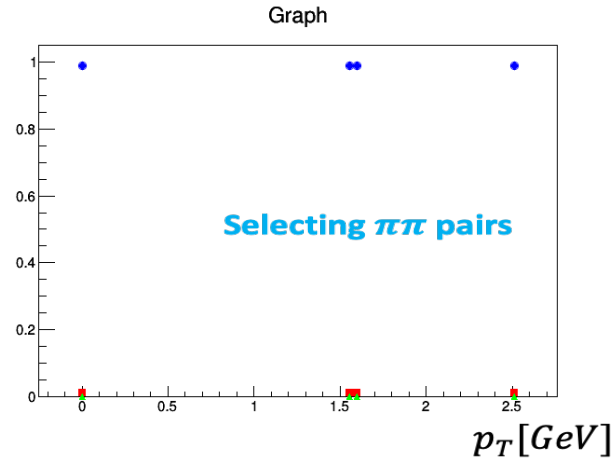
$\pi^+\pi^- \theta_{CM}$ distribution, for $1 < Q^2 < 10$ and Full x



PID Performance

Anselm Vossen

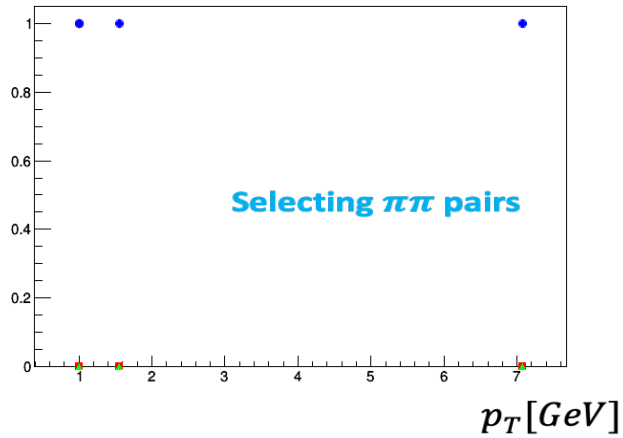
Using 2σ separation



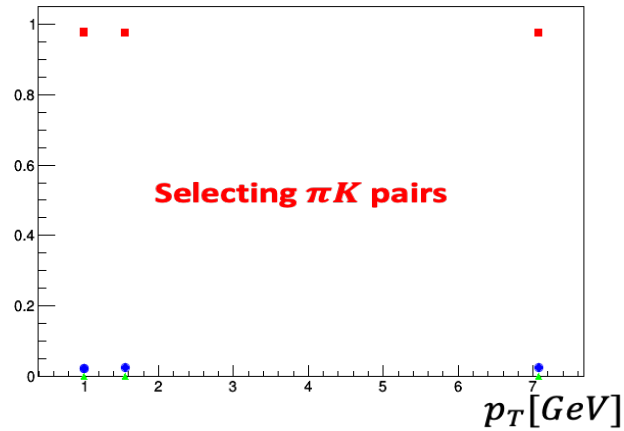
- Fraction of reconstructed $\pi\pi$ pairs
- Fraction of reconstructed πK pairs
- Fraction of reconstructed KK pairs

Using 3σ separation

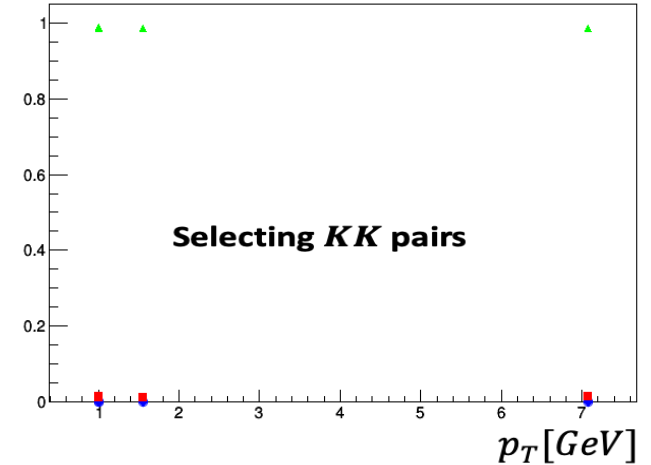
Graph



Graph

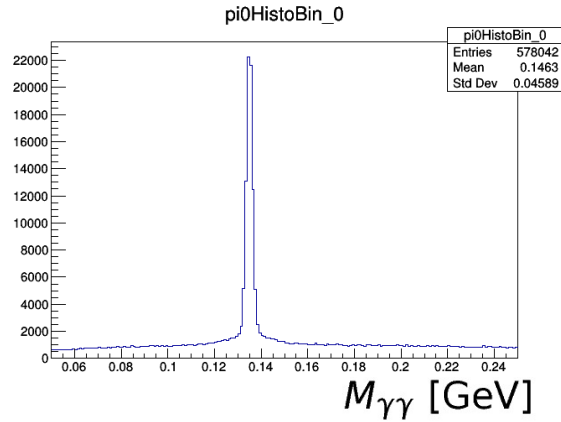


Graph

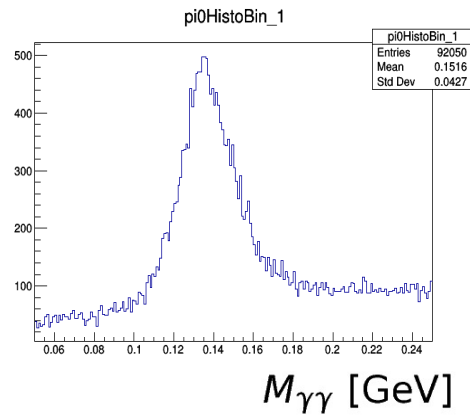


- Fraction of reconstructed $\pi\pi$ pairs
- Fraction of reconstructed πK pairs
- Fraction of reconstructed KK pairs

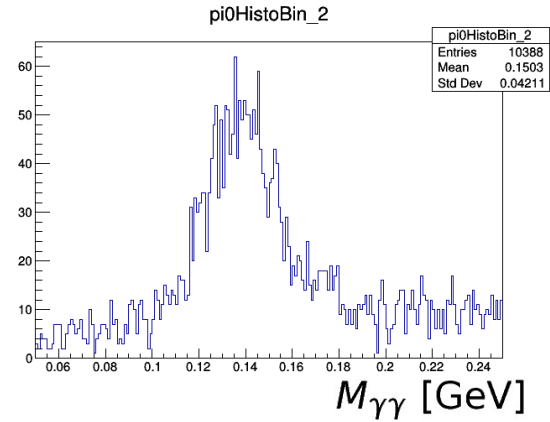
Reconstructing π^0 with $E_\gamma > 200 \text{ MeV}$



$-4.5 < \eta < -1.5$

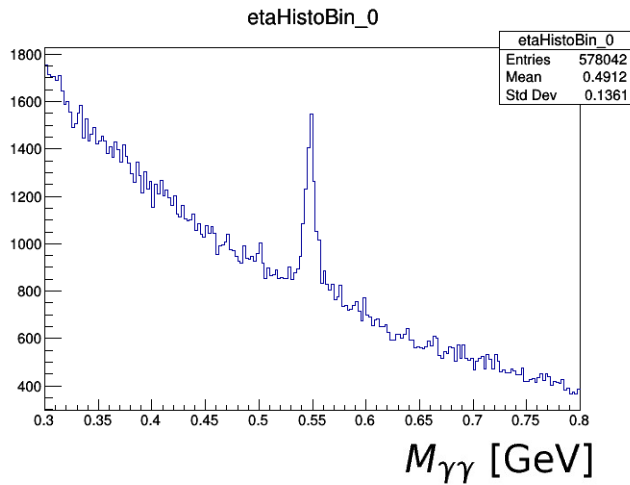


$-1.5 < \eta < 0.5$

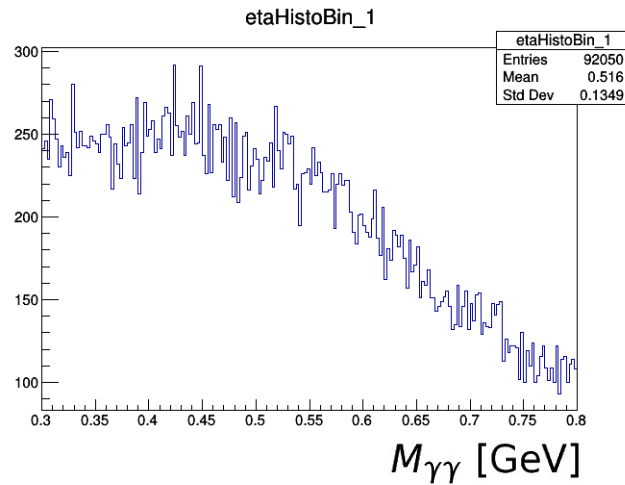


$0.5 < \eta < 4.5$

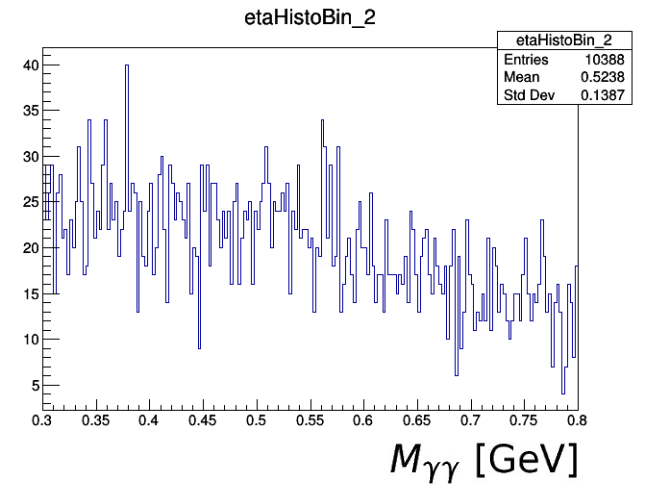
Reconstructing η with $E_\gamma > 200 \text{ MeV}$



$$-4.5 < \eta < -1.5$$



$$-1.5 < \eta < 0.5$$



$$0.5 < \eta < 4.5$$

Summary

- Dihadrons access spin-orbit correlations in hadronization and twist-3 (TMD)PDFs
- EIC simulation studies for SIDIS dihadrons are well underway
- Next Steps:
 - Asymmetry Projections
 - Partial Wave Projections
 - Impacts of p_T cuts
 - Additional dihadron channels, involving neutral pions and kaons
 - Fast simulation impact on dihadron kinematics